

**Evaluation of Microcracking and Chemical  
Deterioration in Concrete Pavements**

**Phase II Progress Report**

**February 28, 1995**

**Iowa DOT PROJECT HR-358  
ERI PROJECT 3711**

Sponsored by the Highway Division of the Iowa Department of  
Transportation and the Iowa Highway Research Board

Iowa Department of Transportation  
Library  
800 Lincoln Way  
Ames, Iowa 50010

**ENGINEERING RESEARCH INSTITUTE**

**IOWA STATE UNIVERSITY**

**ISU-ERI-AMES 95-411**

TA1  
Io8p  
96-402a

**Evaluation of Microcracking and Chemical  
Deterioration in Concrete Pavements**

**Phase II Progress Report**

**February 28, 1995**

**S. Schlorholtz**

**J. Amenson**

**Iowa DOT PROJECT HR-358**

**ERI PROJECT 3711**

**ISU-ERI-95-411**

**Sponsored by the Highway Division of the Iowa Department of  
Transportation and the Iowa Highway Research Board**

"The opinions, findings and conclusions expressed in this publication are those of the authors and not necessarily those of the Highway Division of the Iowa Department of Transportation."

**TABLE OF CONTENTS**

ABSTRACT . . . . .	iii
INTRODUCTION . . . . .	1
RESEARCH APPROACH . . . . .	1
Background . . . . .	1
Equipment . . . . .	10
Cores Available for Analysis . . . . .	11
Other Samples for Analysis . . . . .	12
Sample Preparation . . . . .	12
CURRENT STATUS . . . . .	13
RESULTS AND DISCUSSION . . . . .	13
Basics . . . . .	13
Preliminary Observations . . . . .	15
SUMMARY . . . . .	34
ACKNOWLEDGMENTS . . . . .	34
REFERENCES . . . . .	34

## ABSTRACT

The major objective of this research project is to investigate the chemistry and morphology of portland cement concrete pavements in Iowa. The integrity of the various pavements is being ascertained based on the presence or absence of microcracks, the presence or absence of sulfate minerals, and the presence or absence of alkali-silica gel(s). Work is also being done on quantifying the air content of the concrete using image analysis techniques since this often appears to be directly related to the sulfate minerals that are commonly observed in the pavement cores.

The second year of this project has been spent finalizing the procurement of the research equipment that was necessary for completing this project. Major equipment delays and subsequent equipment replacements have resulted in significant delays. However, all these details have been resolved and the equipment is currently in place and fully operational. The equipment that was purchased for this project can be summarized as follows:

Item	Description	Current Status
1	LECO VP 50, 12 inch diameter variable speed polisher/grinder	Rec'd 8/5/93, fully operational
2	Hitachi S-2460N, environmental (low-vacuum) scanning electron microscope (SEM)	Rec'd 8/26/93, operational but not in compliance as of 2/17/94.  Original SEM replaced with an updated model on 1/24/95; system fully operational on 2/9/95.
3	Link ISIS Microanalysis system with a GEM super ATW Pentafet X-ray detector	Computer system fully operational on 7/7/94. GEM detector delivered and installed on 7/31/94; system is fully operational.

To date, sixty-three concrete specimens have been obtained and are currently ready for analysis. Additional test specimens were obtained from Iowa DOT research project HR-327, entitled "Evaluation of the Chemical Durability of Iowa Fly Ash Concretes." Approximately 20% of the core specimens have been studied in the SEM. Current estimates indicate that the project will be completed on time.

## INTRODUCTION

The following report summarizes the research activities conducted on Iowa Department of Transportation Project HR-358, for the period March 1, 1994 through February 28, 1995.

The objective of this research project is to investigate the chemistry and morphology of core specimens that have been taken from portland cement concrete pavements throughout Iowa. The pavements that were selected for coring have exhibited a wide range of field performance; and hence, this should help to contrast how microstructure relates to the observed performance of field concrete.

The goal of the project is to enhance the ability of engineers to diagnose the reason(s) for materials related failures in concrete pavement systems.

## RESEARCH APPROACH

### Background

Concrete is typically a very durable building material. However, there are a few instances where special precautions must be taken to ensure that it does not exhibit premature deterioration. For instance, when concrete is exposed to cyclical freezing and thawing it is normally desirable to use an air-entraining admixture to increase the durability of the mortar fraction of the concrete. Also, when concrete is to be exposed to soluble salts (sulfates, alkalis, etc.) it is wise to use a mix design that produces a concrete with a very low permeability (i.e., low water/cement ratio), high cement content (using the proper ASTM cement type), and one that incorporates aggregates that are not prone to alkali-induced expansion. However, the deterioration of concrete is still a fact of life. Any composite material like concrete can fail because of a wide variety of different circumstances. The key to understanding and avoiding future occurrences of similar failures is to be able to identify the true cause of the problem, whether it is related to design parameters, materials constraints or construction processes.

Recent field observations of deteriorating concrete pavements in Wisconsin, Minnesota and Iowa have indicated that several different forms of chemical and/or physical attack may have been involved in the degradation process[1,2,3]. The major deterioration mechanisms that have been identified were alkali-aggregate (silicate) reaction (ASR), delayed ettringite formation

(DEF), and freeze-thaw damage. It is pertinent to point out that mixed mode failure (i.e., ASR or DEF coupled with freeze-thaw attack) are much more probable in pavement concrete due to the severe exposure conditions. Each mode of deterioration produces microcracks that grow as the degradation proceeds. Hence, a brief review of the degradation mechanisms seems pertinent at this time. Only a macroscopic perspective will be discussed because the microscopic perspectives have been addressed in a previous report [4].

Alkali-aggregate reactions occur because some types of aggregates react with the alkaline pore solution in concrete to produce a gel. The gel tends to imbibe water and expand. The expansion, which is typically very near (or within) the aggregate particle, eventually causes cracking in the surrounding paste. This process is illustrated in Figure 1. The kinetics of the process (i.e., the time required for the onset of deterioration) are very complicated and researchers are still working to find reliable correlations between laboratory testing and actual field performance. However, many of the aggregates that exhibit sensitivity to alkalis have been (or are currently being) cataloged [6,7]. Cracking patterns produced by some different types of siliceous aggregates are illustrated in Figure 2. Note that many of the aggregates also exhibit internal cracking during the expansion process. Concrete cores that have been extracted from structures suffering from alkali-aggregate reaction, typically exhibit cracking patterns similar to those shown in Figure 3. Note, that the observed cracking patterns may be different due to difference in restraint (reinforcement or adjacent structures), and that the cracking pattern also depends on whether it was induced by the coarse or fine aggregate particles.

Cracking of portland cement based materials due to delayed ettringite formation (DEF) is considerably less well defined than alkali-aggregate reactivity [9]. In fact, some researchers still insist that such a phenomenon cannot occur in concretes subjected to normal curing (for a literature survey on this topic please refer to reference 9). Also, researchers have had difficulty reaching a consensus on the proper terminology to use to describe this deterioration process. For the purpose of this report the terminology proposed by Day [9] will be used. Hence, the term "secondary ettringite" will be used rather than delayed ettringite formation (DEF), to describe the deterioration

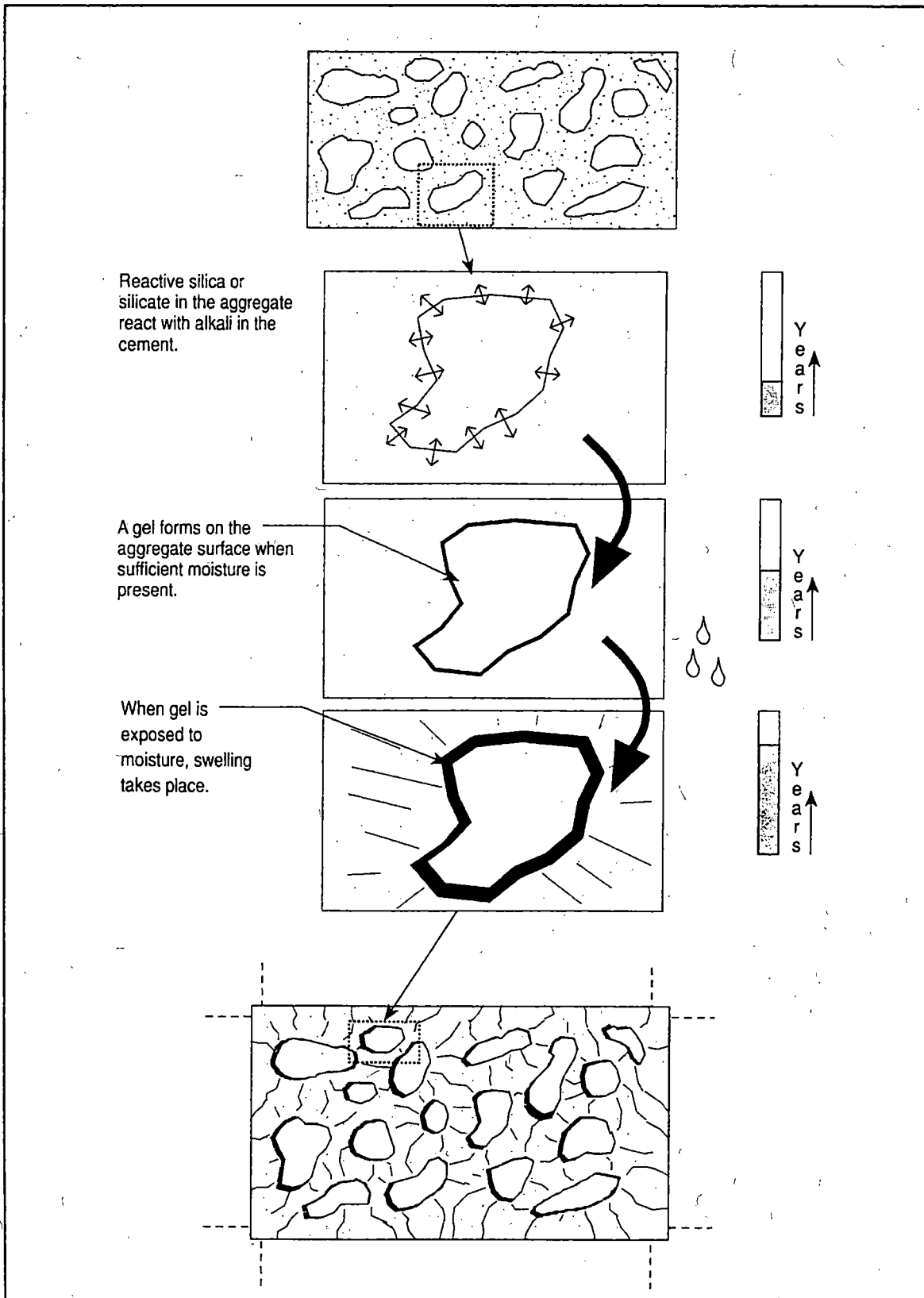


Figure 1. Illustration of alkali-silica reaction in concrete products (adapted from [5]).

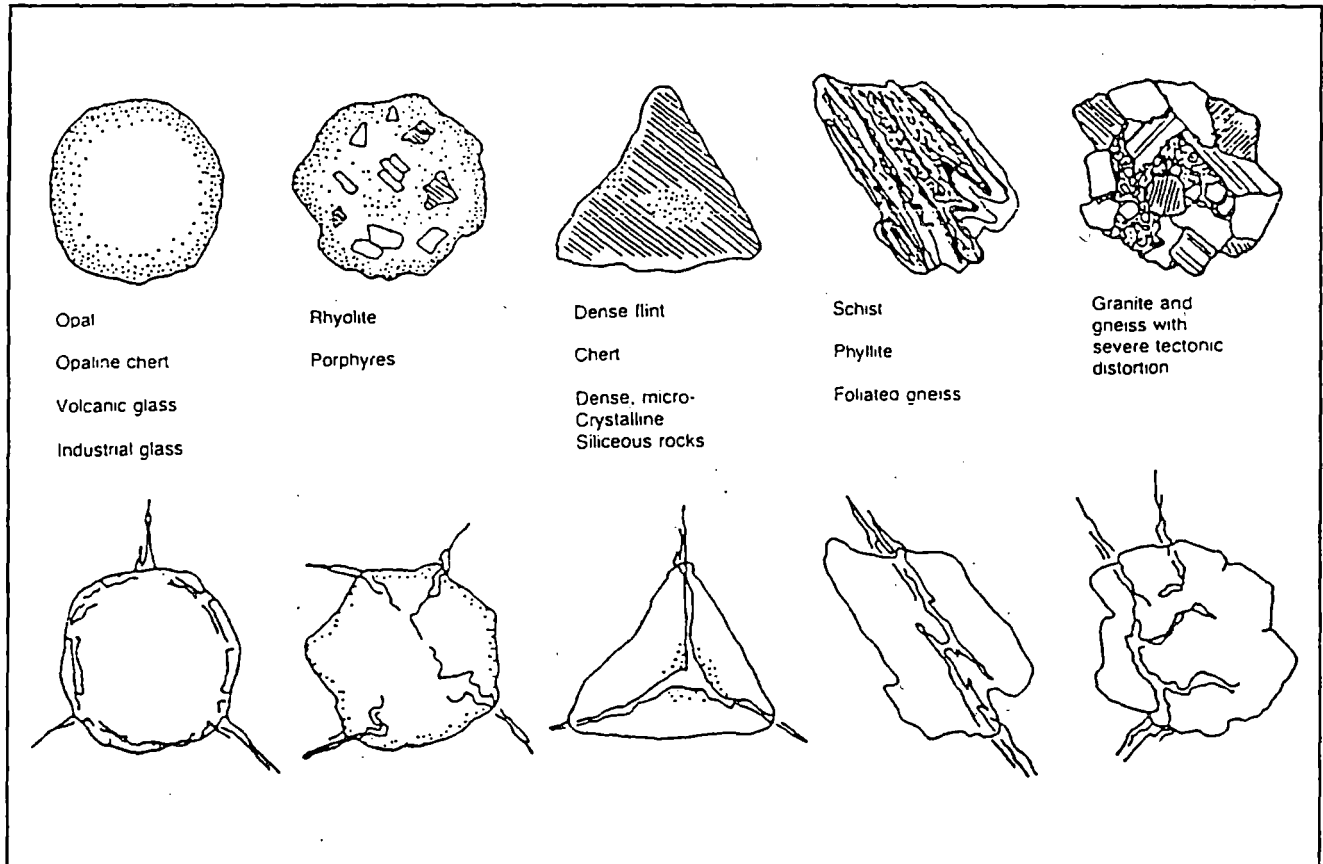


Figure 2. Typical aggregate cracking patterns attributed to alkali-sensitive rock types (taken from [8]).

mechanism in which the growth of ettringite crystals causes cracking in hardened concrete products. The cracking is typically observed several years after construction is completed. This deterioration mechanism is different from normal (external) sulfate attack because the external source of sulfates is not required (see Figure 4). Hence, the overall cracking pattern is slightly different from that shown in Figure 4 (see Figure 5), because the cracking does not originate at the external surface and progress inward. Instead, the expansion occurs on the interior (moist, paste fraction) of the specimen. The chemical product evident in both cases is the same, namely the formation of excessive amounts of ettringite.

Weathering (freezing and thawing) often plays a major role in the deterioration of concrete pavements. This is due to the severe exposure conditions (i.e., continuous wetting and drying coupled with large temperature fluctuations), plus the routine application of deicing salts. Freeze-thaw

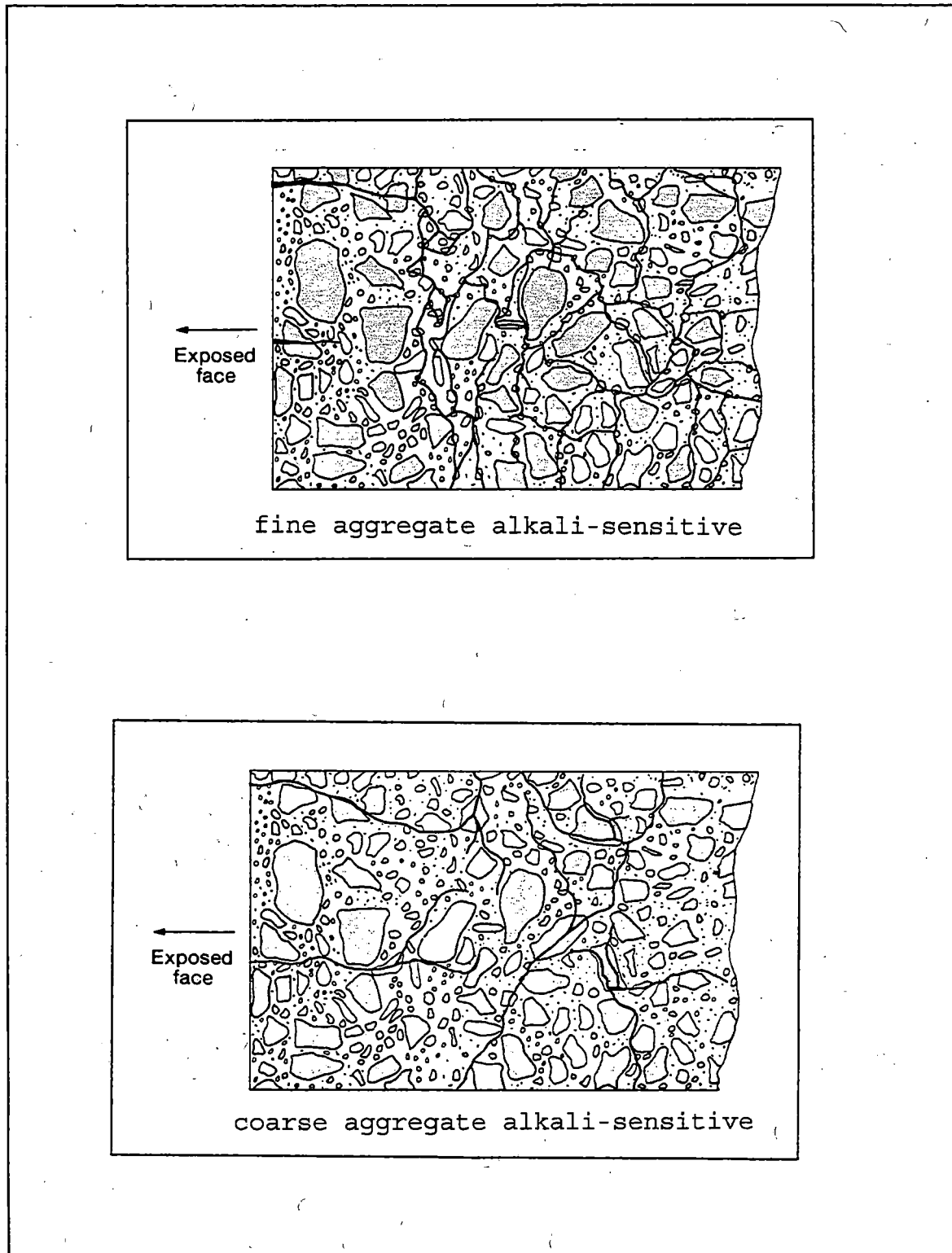


Figure 3. Typical cracking patterns observed in concrete cores extracted from structures containing alkali-sensitive aggregates (taken from [7]).

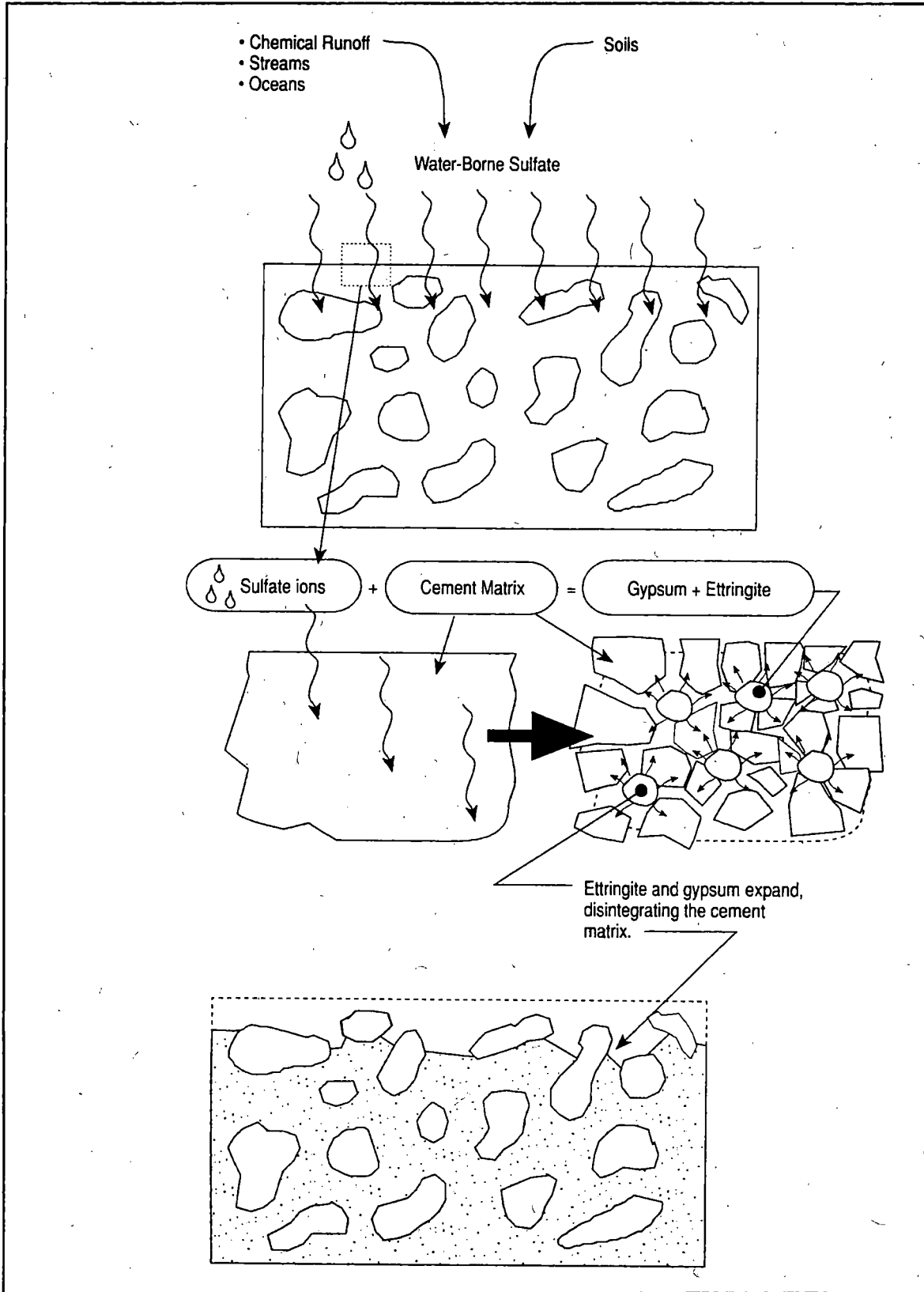


Figure 4. Illustration of external sulfate attack in concrete products (taken from [5]).

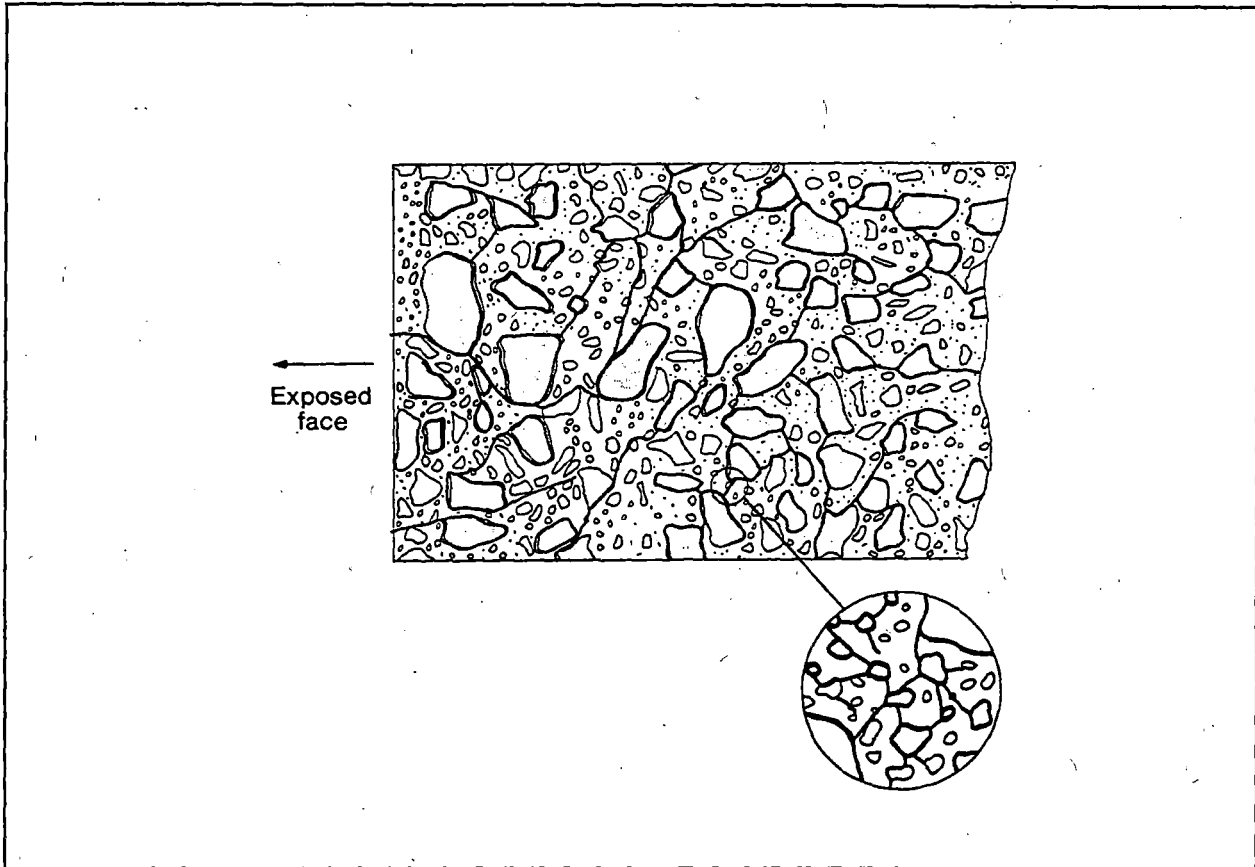


Figure 5. Typical cracking pattern-observed in concrete cores that have experienced internal sulfate attack (taken from [7]).

durability failure (i.e., cracking) can occur in the mortar phase of the concrete or in the coarse aggregate fraction of the concrete. Illustrations of these two failure modes are given in Figures 6 and 7, respectively. The durability of the mortar can be improved considerably by entraining air voids in the concrete. Likewise, selective quarrying and proper materials specifications (based on service record) generally help to avoid coarse aggregate durability failures. The cracking pattern that is typically observed in cores with frost damage is illustrated in Figure 8.

There are several other processes that may cause cracking in portland cement based products. The interested reader should refer to [7] for a general overview of these processes and a description of the cracking patterns that may be observed in field investigations.

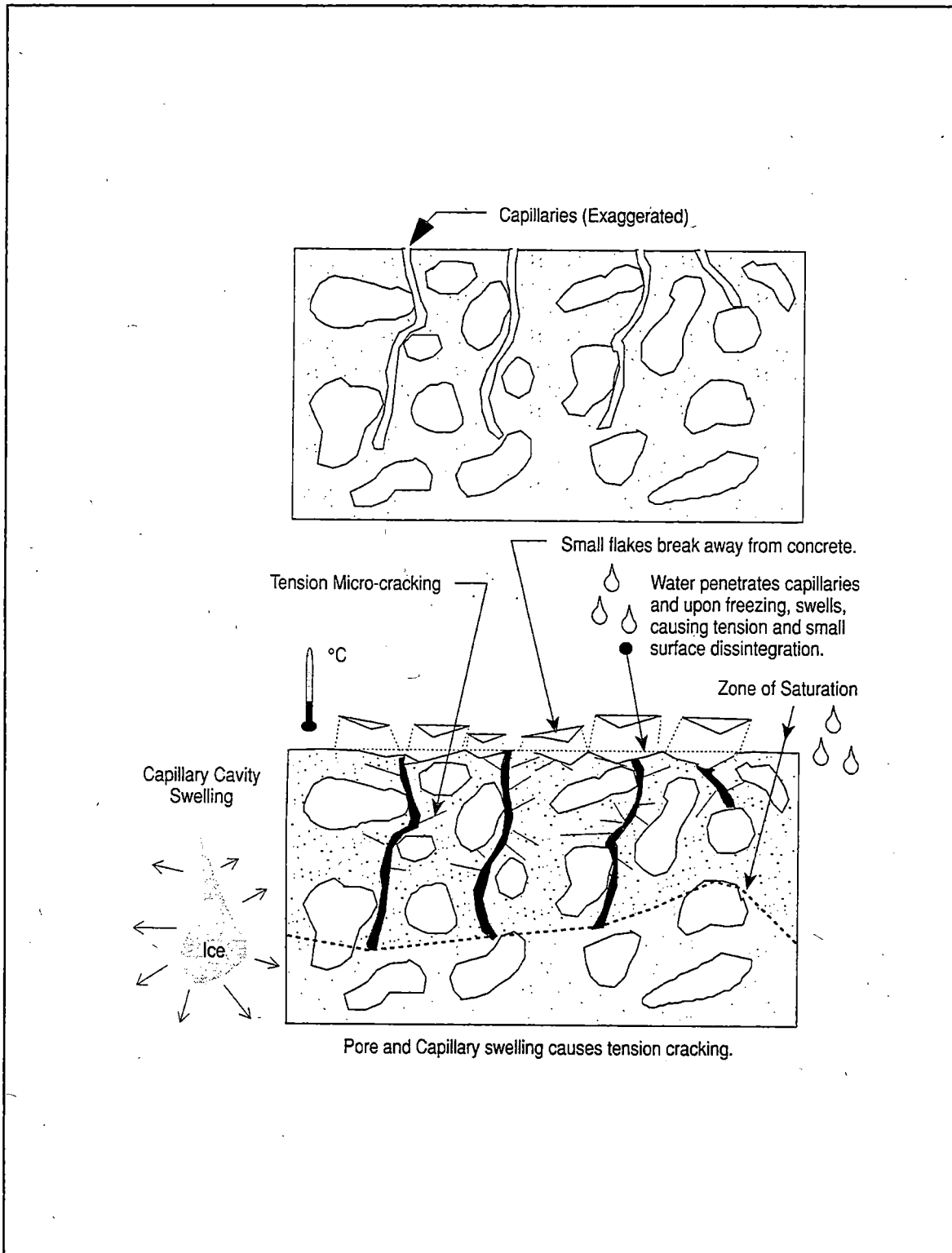


Figure 6. Illustration of freeze-thaw damage in the mortar fraction of a concrete product (taken from [5])

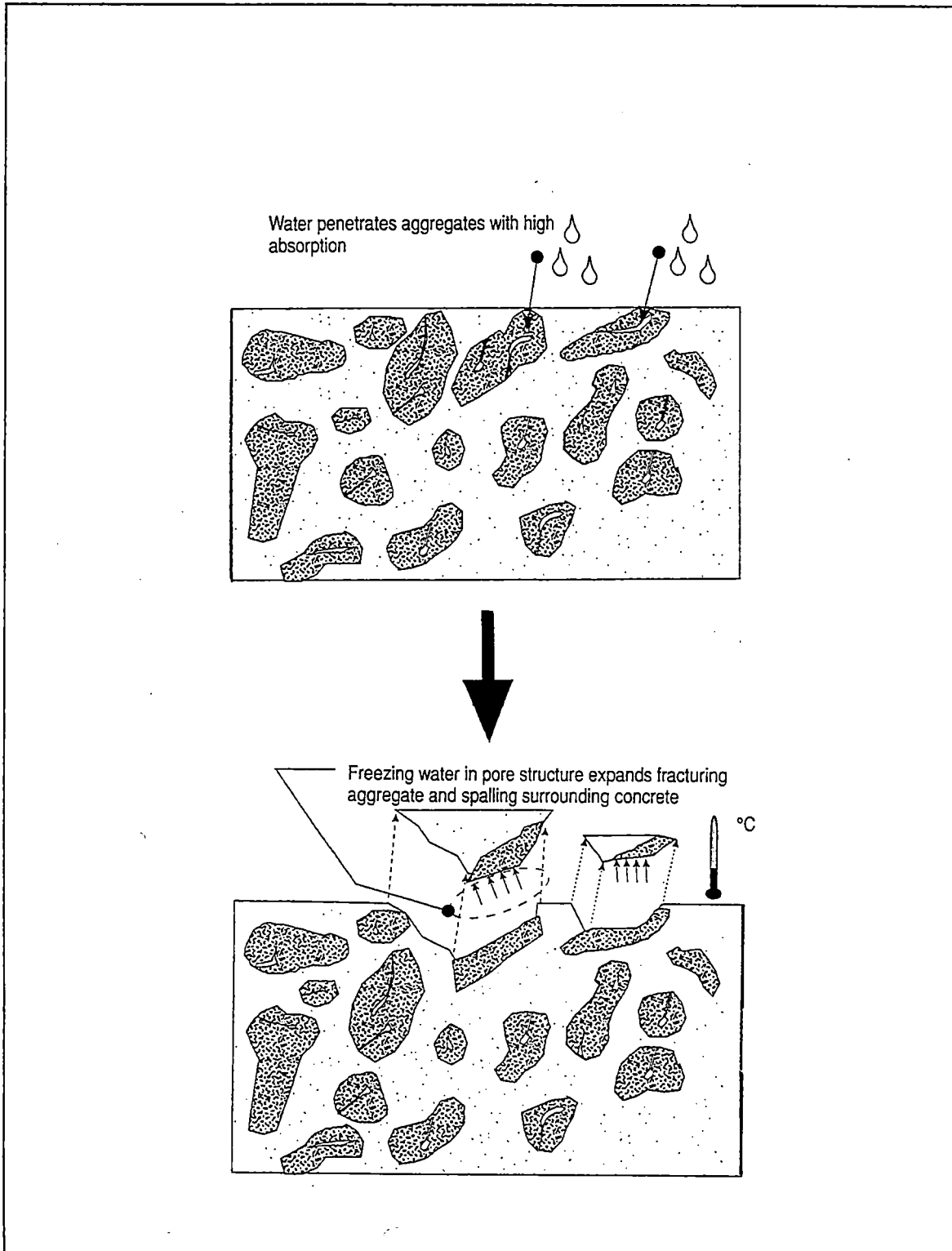


Figure 7. Illustration of freeze-thaw damage that originates in the coarse aggregate fraction of concrete (taken from [5]).

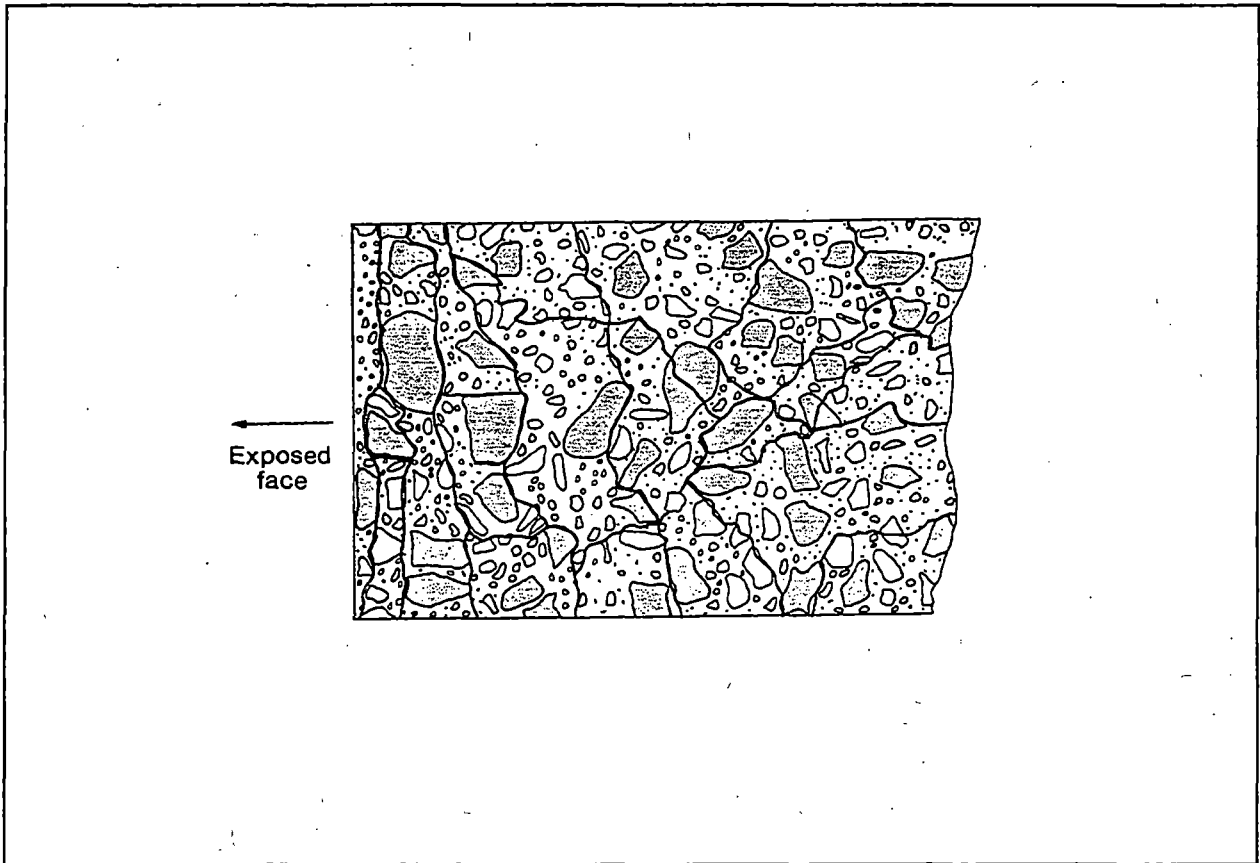


Figure 8. Typical cracking pattern observed in concrete cores extracted from structures exhibiting freeze-thaw damage (taken from [5]).

### Equipment

Three major pieces of equipment were purchased for this research project. The new equipment included: (1) a low vacuum scanning electron microscope (SEM); (2) an energy dispersive X-ray analyzer with an image analysis system; and (3) a variable speed grinder/polisher with a 12-inch diameter wheel. Only the SEM upgrades will be described in this report.

A Hitachi S-2460N, variable pressure SEM was purchased for the project. This SEM was selected because it would accept large specimens (up to 6-inches in diameter) and had a stage movement capable of traversing a four inch specimen. The SEM can be operated at pressures ranging from 0.01 to 2 Torr, in the variable pressure mode. The "variable pressure" mode allows researchers to analyze difficult specimens (like portland cement mortar) or

concrete) in their natural state without the tedious sample preparation techniques that are normally mandatory for conventional scanning electron microscopes [10,11].

The first scanning electron microscope was delivered in late August of 1993. However, it was not in compliance with bid specifications and was exhibiting frequent maintenance problems by the end of the first year of the project. Hence, this microscope was replaced with an equivalent model (an upgrade, still denoted as model S-2460N) that had several additional features (see Table 1). The microscope is now fully functional and it will certainly meet the requirements of this research project.

Table 1. Description of additional features on the S-2460N SEM.

Item	Original SEM	Current SEM
Resolution	4.0nm (high vacuum) 6.0nm (low vacuum)	4.0nm (high vacuum) 6.0nm (low vacuum)
Magnification	20 to 200,000X (41 steps)	10 to 200,000X (65 steps)
Accelerating voltage	0.5 to 25kV (39 steps)	0.3 to 30kV (62 steps)
Auto start function (with SEM setup memory)	not available	standard
Digital beam current control	not available	standard

#### Cores Available for Analysis

Core specimens were drilled from a variety of different portland cement concrete pavements across Iowa. The core samples were taken by Iowa Department of Transportation (IDOT) personnel and then transported to the Materials Analysis and Research Laboratory (MARL) at Iowa State University, for specimen preparation and analysis.

The various pavement cores were assigned priority numbers, ranging from 1 through 6, at a subsequent meeting with IDOT engineers and geologists. Priority numbers were assigned to indicate the order that the samples should be analyzed (highest priority = 1, lowest priority =6).

Table 2. Summary of cores taken for this project.

Priority Number	Description	Number of Cores
1	Cores from the Materials Quality Task Force study at the Iowa DOT	6 cores 2 beams
2	U.S. 520 in Webster County	12
3	I-35 in Story County	8
4	I-80 in Dallas County	4
5	Bettendorf street in Scott County	4
6	Assorted cores from Louisa, Madison, Hamilton, Union and Buchanan Counties	25

### Other Samples for Analysis

A wide variety of mortar bar specimens and several concrete beam specimens were also available for analysis. All of the mortars and concretes were taken from a chemical durability research project that had recently been completed (HR-327). Hence, all of the mortars and concretes were proportioned, mixed and cured in a laboratory environment. All of these samples have been exposed to very severe environments which should have accelerated the alkali silica reaction or sulfate deterioration processes. Also, the various test specimens had been monitored for various physical properties (i.e., length change, etc.) as a function of exposure time. This should allow a more quantitative evaluation of the level of deterioration that is present in the mortar fraction of the specimens.

### Sample Preparation

Sample preparation for the low-vacuum scanning electron microscope used in this study, is considerably simpler than the techniques that are commonly employed for conventional scanning electron microscopes because there is no need to coat the sample with a conductive film. Several different sample preparation methods have been used during different stages of this project. They included fractured surfaces, cut surfaces, ground surfaces and thin sections. The method that was most commonly employed in this project consisted of: (1) sawing off a section of the concrete core (diamond blade, propylene glycol used as a coolant); (2) rinse off the propylene glycol using tap water; (3) grinding the sample surface flat by using fixed grit paper and the 12 inch grinding/polishing wheel described earlier in this report (grit

sizes listed in Table 3, water used as a lubricant). This sample preparation method is very similar to the method that is commonly used to prepare specimens for air void analysis by standard ASTM procedures [6].

Table 3. Grinding and polishing procedure for the concrete cores.

Step	Current method grit size (micron equiv.)	ASTM C 457 (see [6]) grit size (micron equiv.)
1	180 (70 $\mu$ m)	100 (150 $\mu$ m) optional
2	320 (30 $\mu$ m)	220 (75 $\mu$ m)
3	600 (17 $\mu$ m)	320 (35 $\mu$ m)
4	800 (12 $\mu$ m)	600 (17.5 $\mu$ m)
5	1200 (2 to 5 $\mu$ m)	800 (12.5 $\mu$ m)
6	optional 1 $\mu$ m diamond paste	optional 5 $\mu$ m Alumina

### CURRENT STATUS

The work plan and activity schedule that was proposed for this project (see Table 4) had to be altered because of problems that were experienced in obtaining major equipment items (task 1 items). Multiple delays in the delivery date for the GEM X-ray detector, coupled with recurring technical problems on the SEM, have delayed the activity schedule by about one year. These discrepancies have been resolved and the activity schedule has been updated to reflect the delays.

### RESULTS AND DISCUSSION

#### Basics

Preliminary results from this study will be discussed in detail. However, due to the nature of the data collected in this research project (i.e., pictures or images), it is difficult to display the results in a text-based report. Only details that are clearly evident will be presented in this report. Also, since this report has been published without using color, it lacks many of the sophisticated

Table 4. Updated activity schedule for this project.

Task #	Proposed Work Plan	Status (and comments)
1	Get quotes and purchase major equipment items	task completed
2	Get quotes and purchase a grinder/polisher	task completed
3	Prepare concrete samples for ASR study using hot alkali baths	task eliminated
4	Fine tune specimen preparation techniques	task about 90% complete (still developing a reliable method for air content determinations)
5	Prepare and analyze calibration samples	task about 50% complete (priority reduced so that more core specimens can be studied)
6	Get cores from IDOT	task completed
7	Cut cores into sections and prepare for analysis	task completed (however, we are currently cutting some cores longitudinally for additional work)
8	Analyze specimens and archive the test results	task about 20% complete
9	Prepare reports	first and second progress reports have been completed

image processing techniques that can be used to enhance and clarify subtle details. These techniques are available and can be used to manipulate the digital data; however, publishing costs prohibited their use in this report.

As mentioned above, two types of information have been collected in this project. First, the macroscopic and microscopic features from each core have been collected by means of pictures. And secondly, the chemistry of the core specimens has been investigated by collecting digital X-ray maps of

various features that were observed in the pictures. Obviously, as the title of this research project suggests, the regions of interest will normally contain cracks.

The pictures consist of the normal (analog) format and a more modern, computer readable format (digital, this format was available only for work conducted using the SEM). The analog format currently offers more resolution (about 2000 by 2000 lines per picture) than the digital format (digital images can be collected at 256 by 256 pixels, 512 by 512 pixels or 1024 by 1024 pixels). However, the digital format will surely be the media of the future because: (1) computer storage media costs are falling rapidly,; (2) the resolution of digital images is constantly being increased (second source vendors already boast 4096 by 4096 pixel images); and (3) the images can be manipulated (i.e., magnified or processed using image analysis) and cataloged (e.g. an image database) using less resources than is required for conventional pictures. For the purpose of this research project both media formats have been used. Typically, pictures were taken using Polaroid Type 55 film because it has a negative that can be used for enlargements. The digital images were normally collected using the high resolution (1024 by 1024 pixels) mode; however, some lower resolution images were also collected.

The Link ISIS program SPEEDMAP was used to collect the digital X-ray maps for this project. This particular program allows researchers to collect information on 30 different elements, simultaneously. The major elements of interest in this project were carbon (C), oxygen (O), sodium (Na), magnesium (Mg), aluminum (Al), silicon (Si), sulfur (S), chlorine (Cl), potassium (K), calcium (Ca) and iron (Fe). Occasionally, after special treatments, other elements were also measured (i.e., uranium). Digital X-ray maps were normally collected at a resolution of 256 by 256 pixels; however, occasionally higher resolution maps were collected (512 by 512 pixels).

### Preliminary Observations

Mortar bar specimens containing pyrex glass aggregate will be used to illustrate how the SEM technique can be used to document the presence of alkali-silica gel. The mortar bar specimens that were investigated contained a moderate alkali cement (0.76% equivalent sodium oxide content). Some of the specimens also contained Council Bluffs fly ash (high-calcium, Class C). All of the test specimens had expanded between 0.5% and 0.7% in the alkali-

aggregate reactivity tests that had been conducted under research project HR-327 [4].

Alkali-silica related cracking is shown in Figure 9. This particular specimen contains only pyrex glass aggregate and a moderate alkali cement. Note in Figure 9, that the upper left always contains a backscattered electron image of the region that has been mapped. Backscattered electron images are sensitive to atomic number; and hence, heavier elements appear brighter. The remaining images each display an individual element (sodium, silicon, sulfur, potassium or calcium in this instance). The cracks evident in the aggregate particles, have been filled with a material enriched with potassium (note the bright areas in the potassium image, see the lower left of Figure 9). The material filling the cracks was also composed of silicon and sodium, plus only a small amount of calcium. This material fits the description of alkali-silica gel (note, that the term "alkali-silica gel" is used generically, and it commonly describes materials with a rather wide range of chemical composition). In this instance, most of the gel has remained within the boundary of the aggregate particle. This information indicates that the documentation of alkali-silica gel can be directly related to the observation of alkalis, plus the proper associated elements, in the cracked aggregates. Quantification of the chemical composition of the gel is currently being studied.

Field studies often make use of the uranyl acetate fluorescence method to obtain preliminary identification of alkali-silica gel [12]. This technique was evaluated to see if it would simplify the routine identification of alkali-silica gel during SEM analysis. Hence, mortar bar specimens containing pyrex glass, moderate alkali cement and 22.5% Council Bluffs fly ash were treated with uranyl acetate as described in reference 12. Figures 10, 11 and 12 illustrate the results of the experiment. At low magnification (30X), the treatment appears to tag several features (see the uranium map in the lower left of Figure 10, note that uranium makes the features brighter because it is a heavy element). Increasing the magnification to 250X (see Figure 11), reveals some alkali-silica gel between two adjacent aggregate particles. The gel exhibits cracking (? due to drying) and contains the appropriate elements. However, the treatment also tended to tag air voids (see Figure 10) and often failed to tag the gel present in the cracked aggregate particles (see Figure 12). Hence, the method requires considerable refinement before it can be used routinely in this research project. This study has also raised a fundamental question

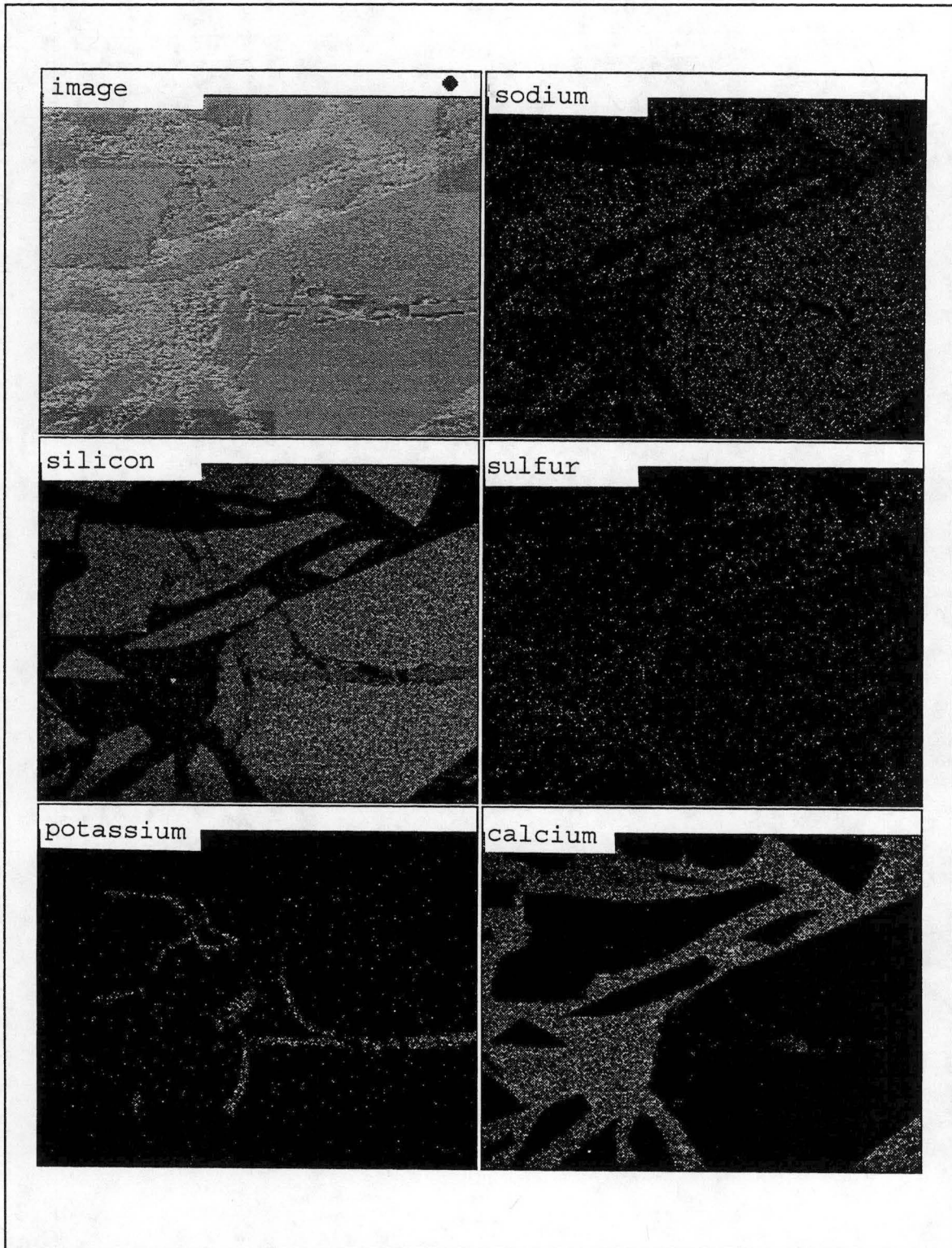


Figure 9. Digital image and X-ray map (magnification =100X) of a mortar bar specimen containing pyrex glass aggregate. Note how cracks mimic the bright areas in the potassium map.

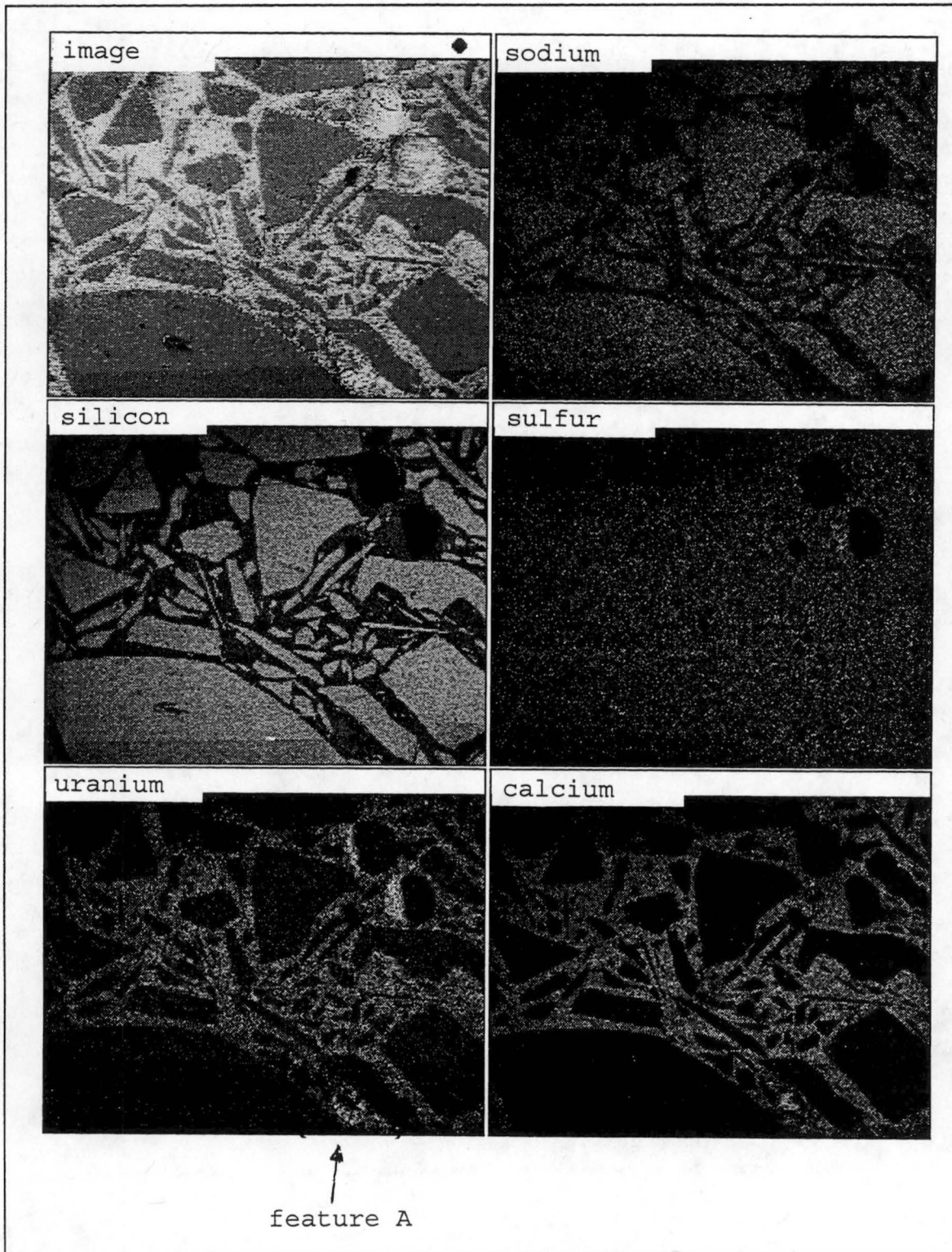


Figure 10. Digital image and X-ray map (magnification =30X) of a mortar bar specimen containing pyrex glass aggregate. This specimen was treated with uranyl acetate to enhance the ASR gel (note the bright regions on the uranium map).

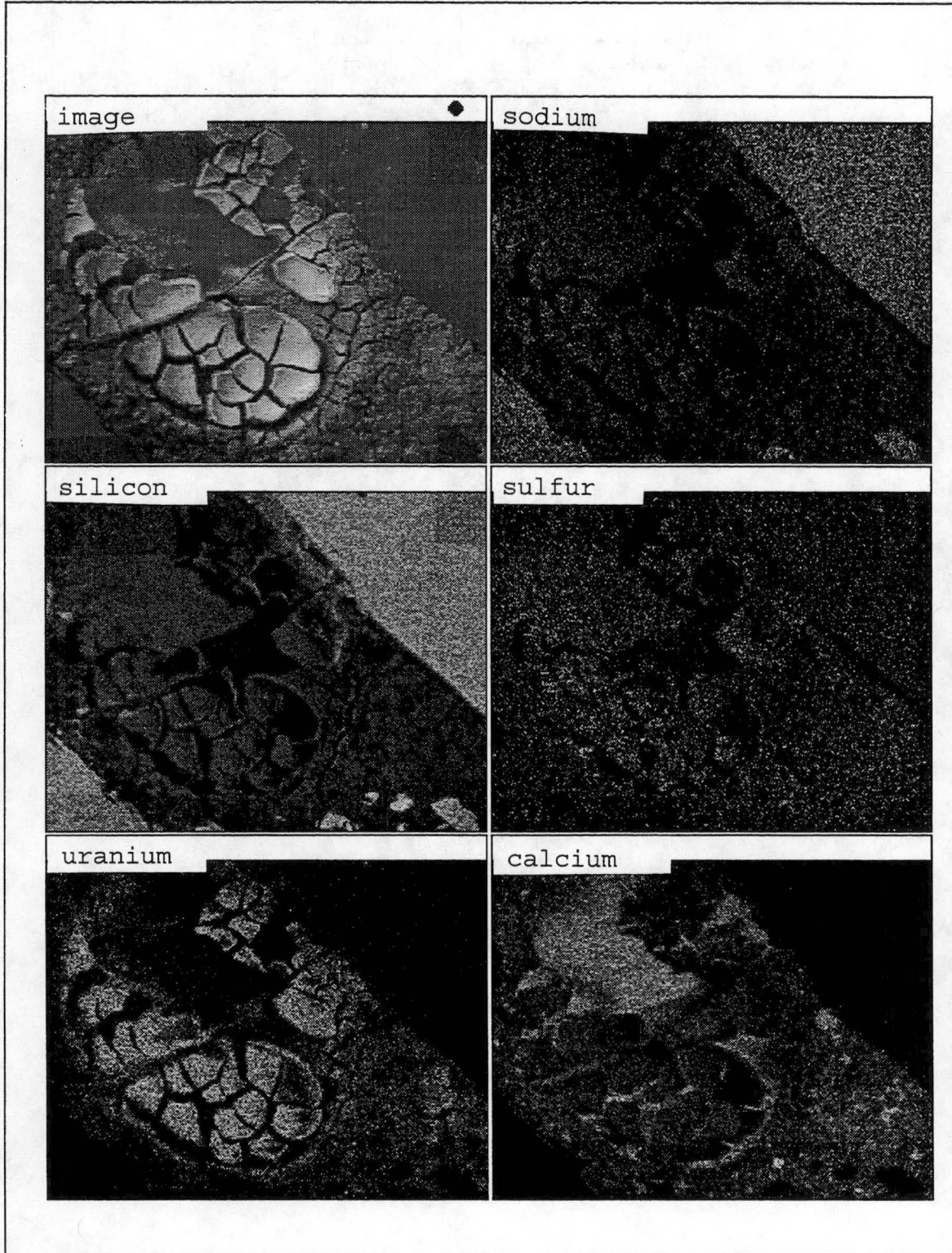


Figure 11. Digital image and X-ray map (magnification =250X) of feature A in Figure 10. This feature is ASR gel between two aggregate particles.

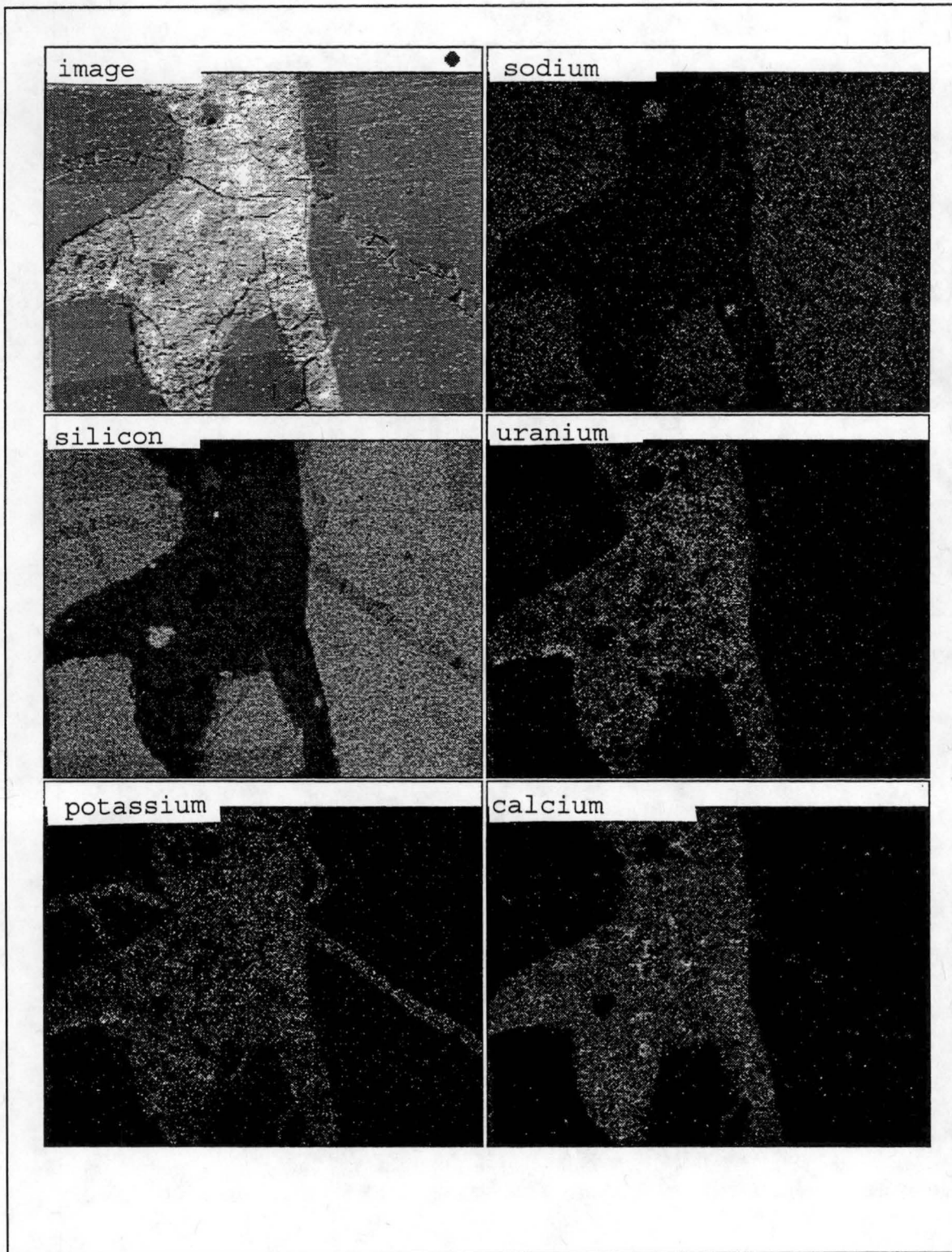


Figure 12. Digital image and X-ray map (magnification =250X) of another region of the specimen described in Figure 10. Note how the uranium map fails to reveal the cracks in the aggregate that are filled with alkali-silica gel (compare to the potassium image).

concerning the mechanism by which the gel is tagged (i.e., "the uranyl ion substitutes for alkali in the gel" [12]). Why is the uranium content so high in the paste fraction and nearly absent in the gel-filled cracks of the aggregate particles? Research is needed to answer this question.

Alkali-silica gel has only rarely been observed in the concrete cores that are being studied for this research project. However, this comment must be considered as "preliminary" because many cores still need to be subjected to detailed investigation. Most commonly, the alkali-silica gel has been observed near shale particles in the fine aggregate fraction of some of the concrete cores. For example, highway 175 has exhibited some areas that clearly contain alkali-silica gel (see Figures 13 and 14). The gel originated from shale particles that were moistened during the sawing and grinding process. Not all of the shale particles have exhibited the formation of alkali-silica gel. However, nearly all of the shale particles exhibit cracking that is evident in both the particle and the adjacent region of cement paste (see Figure 15, this core was taken from highway 520). The cracking rarely extends large distances through the concrete specimen.

Many of the cracks that are routinely observed in the concrete core specimens appear to be open, and thus, have no apparent material filling the cracks (see Figures 16, 17 and 18). Often, the general cracking pattern tends to go around the aggregate particles and through the cement paste and air voids. Little aggregate related cracking is apparent in the core specimens that have been studied to this point.

One feature that is common in many of the concrete cores is the presence of sulfate minerals in the entrained air voids, this is illustrated in Figure 19. The digital X-ray map of the region is shown in Figure 20. The chemical composition of the material in the air voids is often quite close to that which is characteristic of ettringite and the material typically exhibits a fibrous morphology. Experts indicate that this observation is not uncommon [6, 8, 13]. Most common petrographic examination guides also suggest that investigators should document these features because they may be important to understanding the deterioration mechanism.

The amount of void filling that was observed varied considerably from sample to sample. Some of the samples had few air voids that were completely filled (e.g. highway 175), while others had nearly all air voids smaller than 100 microns completely filled. In extreme cases air voids as large as 250

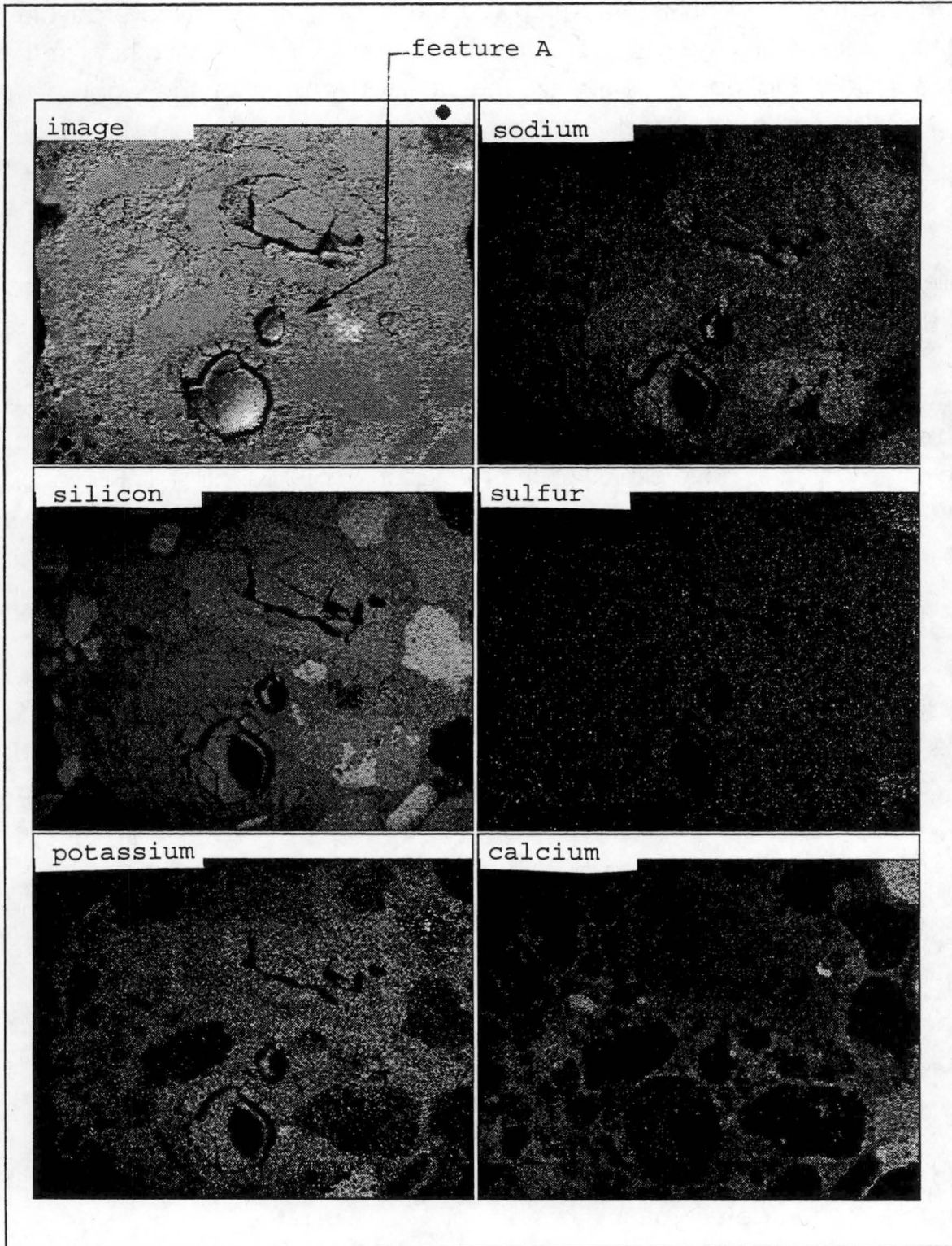


Figure 13. Digital image and X-ray map (magnification =30X) of a region of a concrete core taken from highway 175. The shale particle (upper center) has exuded alkali-silica gel which has filled some voids.

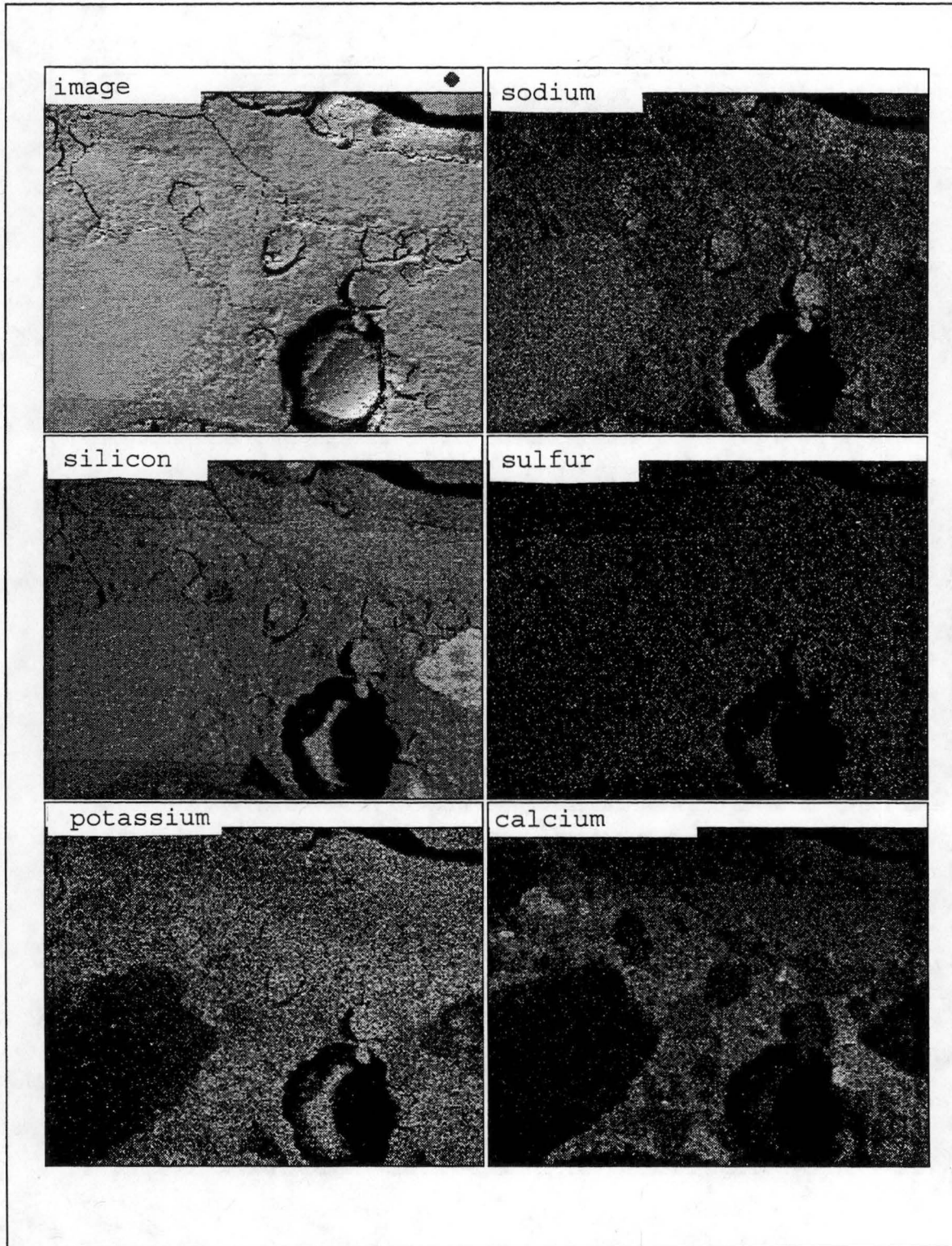


Figure 14. Digital image and X-ray map (magnification =100X) of feature A in Figure 13.

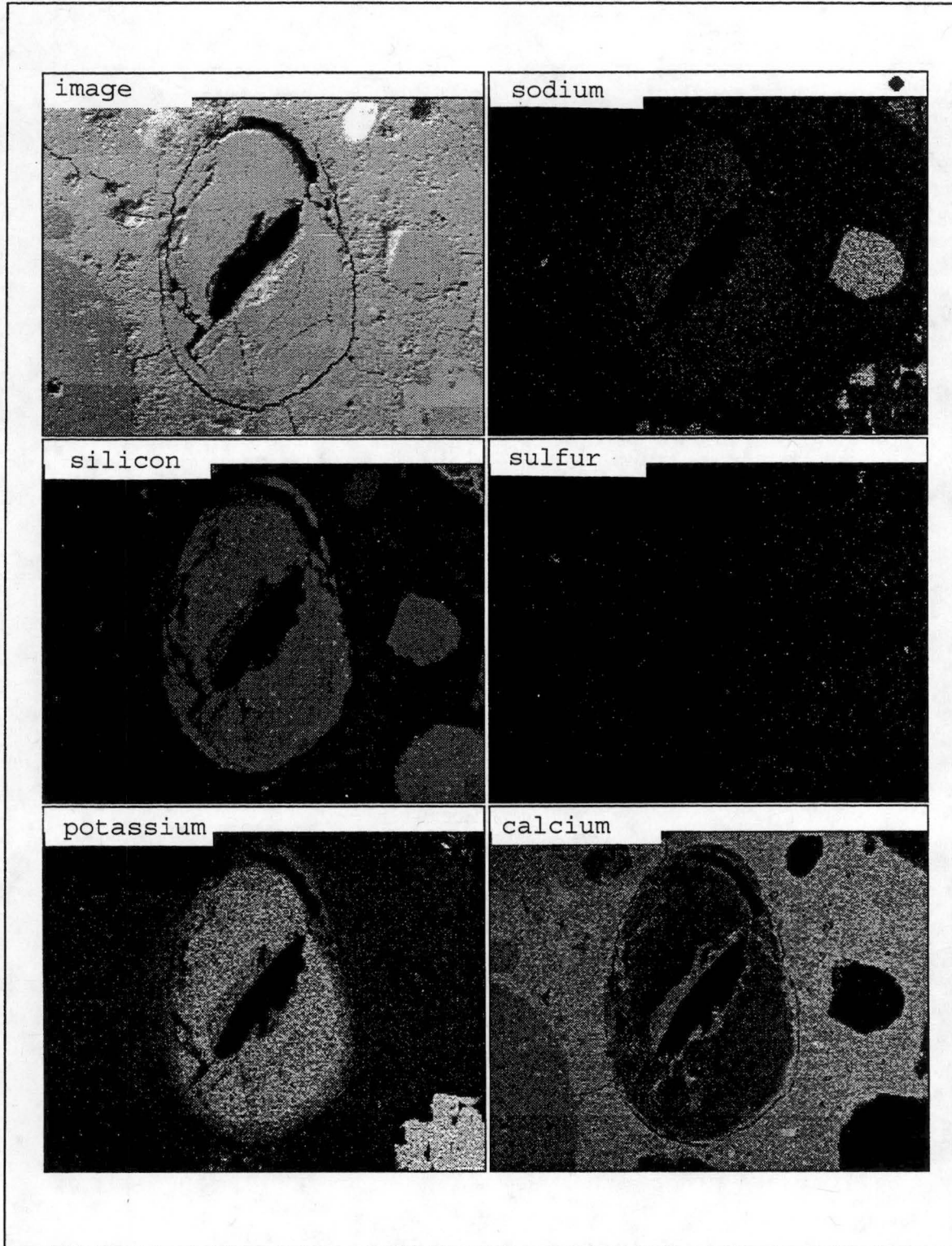


Figure 15. Digital image and X-ray map (magnification =30X) of a shale particle in a core taken from highway 520. Little evidence of ASR gel surrounding shale.

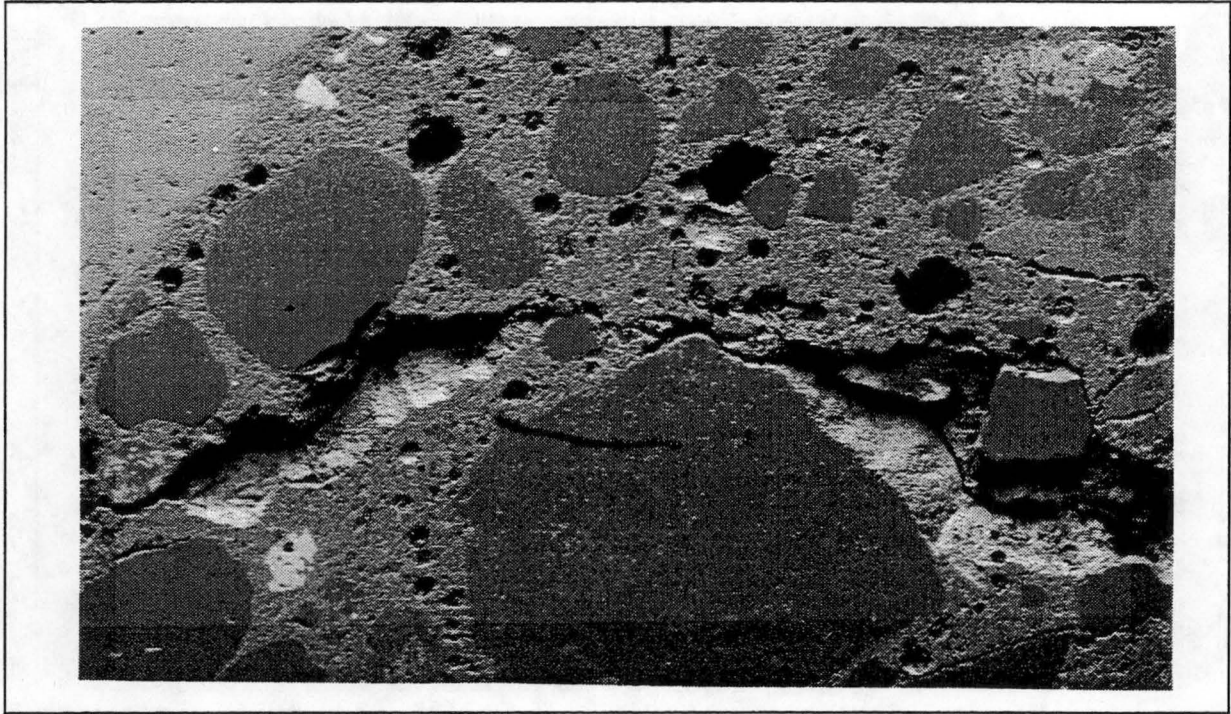


Figure 16. Digital image (magnification =18X) of a region of a concrete core from I-35. Note large crack in paste with few cracked aggregates.

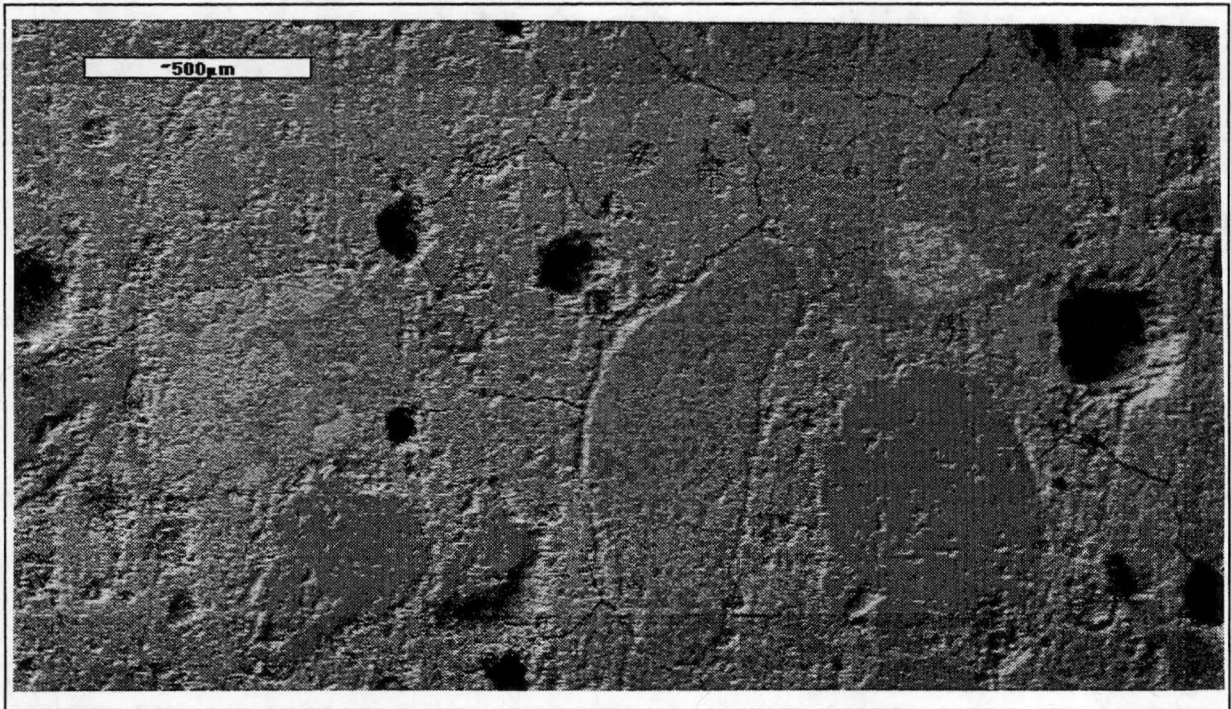


Figure 17. Digital image (magnification = 30X) of a region of a concrete core taken from highway 520. Note cracks in paste with few cracked aggregates. Also, note the filled voids.

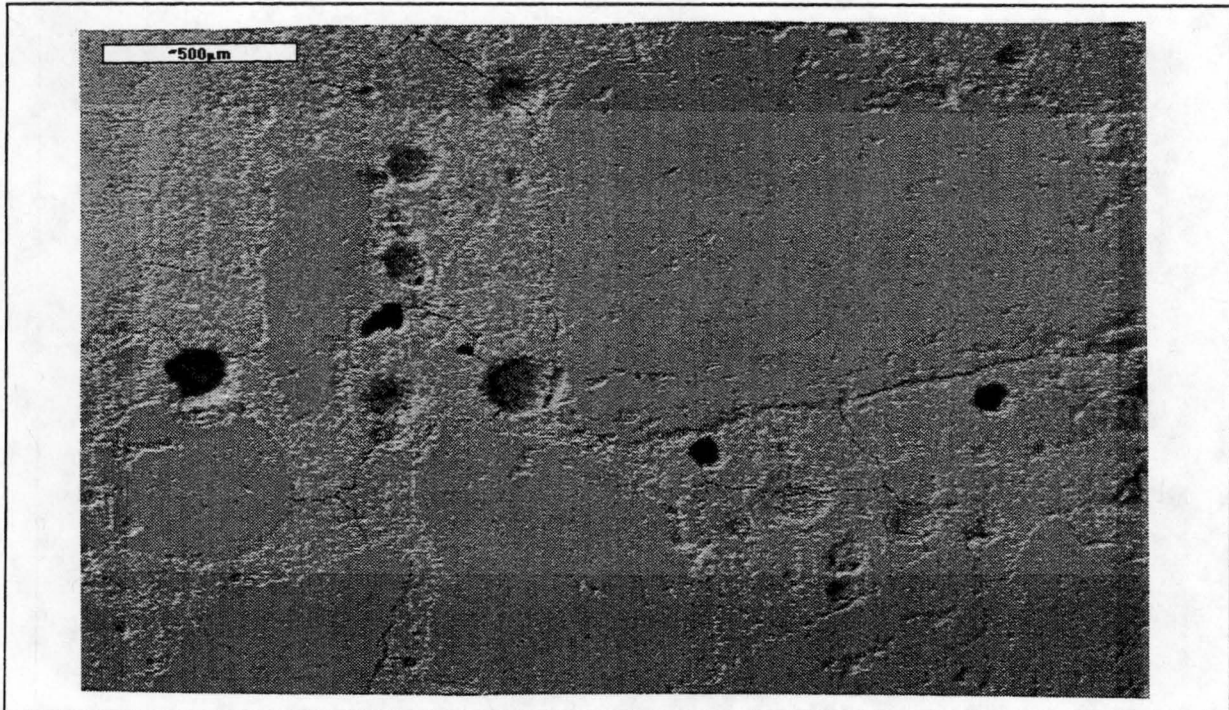


Figure 18. Digital image (magnification = 30X) of a region of a concrete core from I-80. Note cracks in paste with few cracked aggregates.

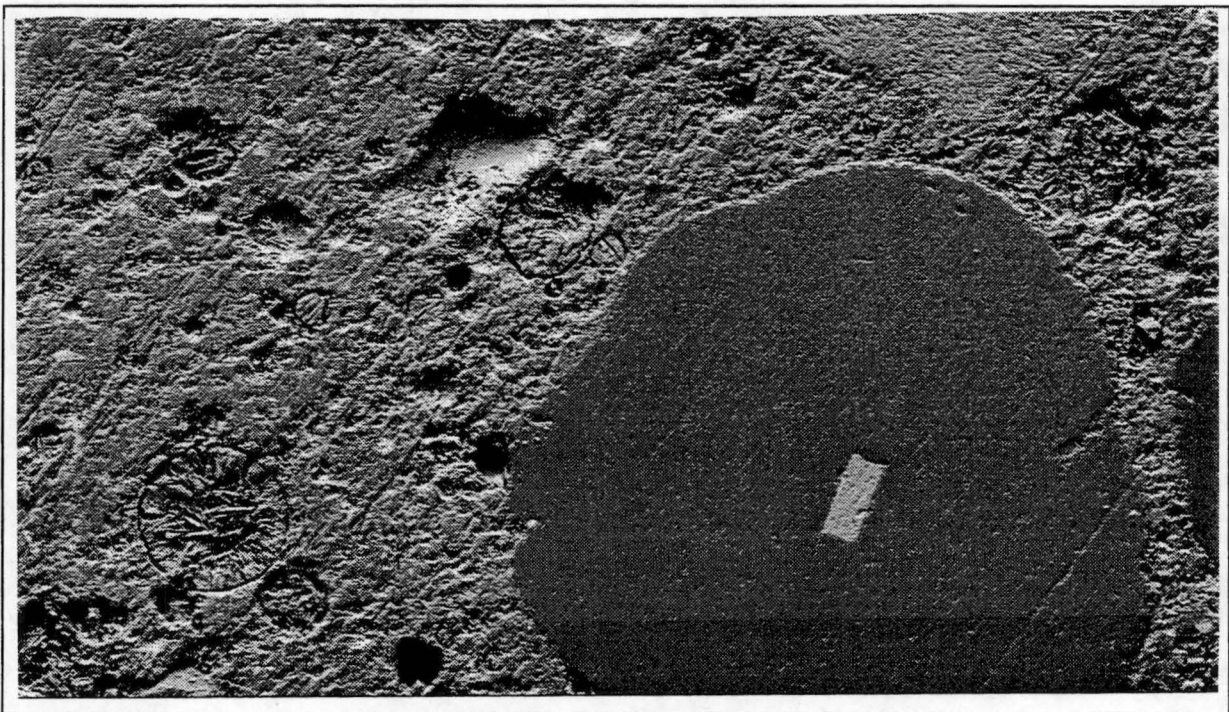


Figure 19. Digital image (magnification = 100X) of a region of a concrete core taken from I-35. Note how the voids have been nearly filled with sulfates.

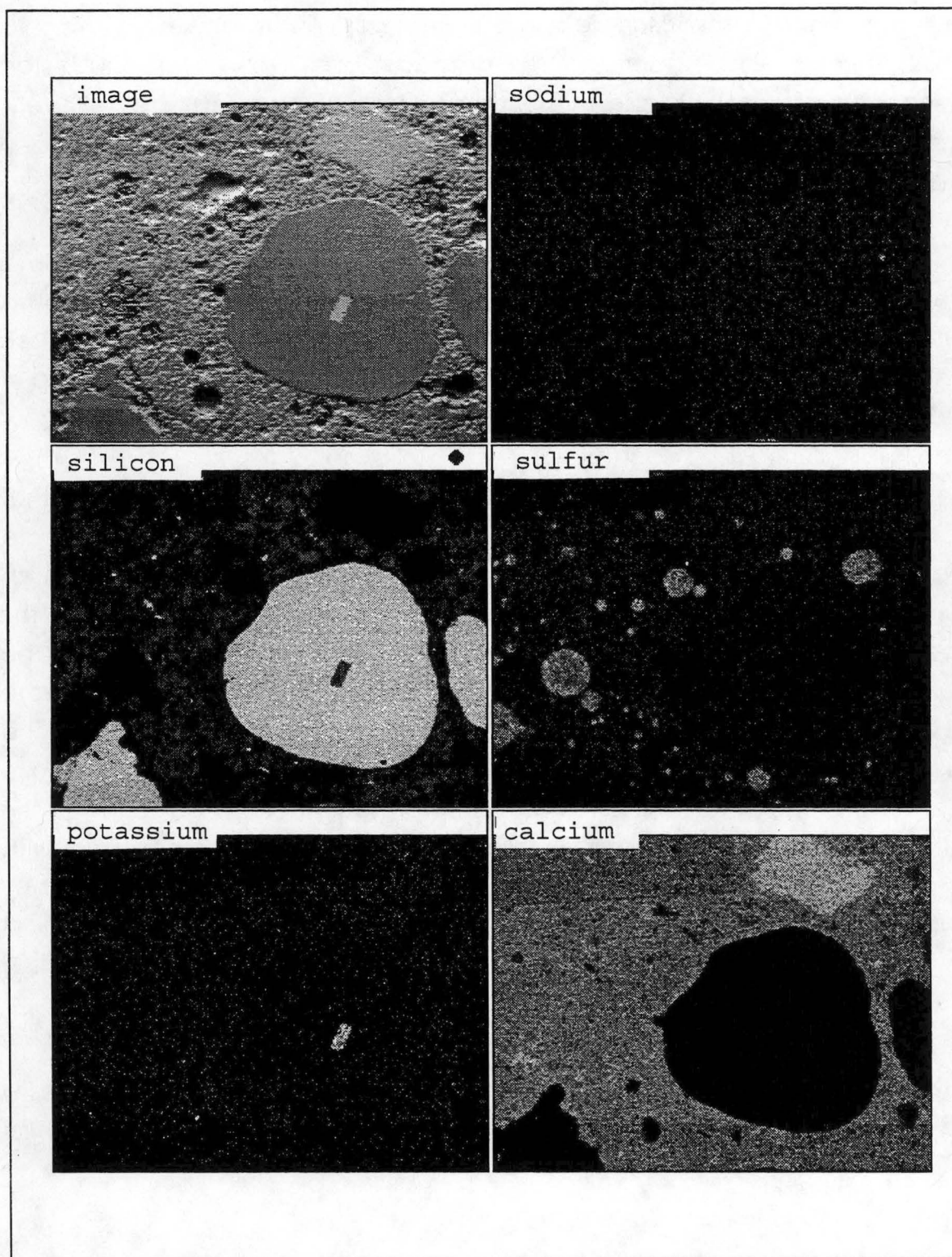


Figure 20. Digital image and X-ray map (magnification =100X) of the region shown in Figure 19. Note how voids are filled with sulfates, not alkalis or silicates.

microns have been completely filled. Hence, void filling occurred on both a macroscopic and a microscopic level. This is best illustrated by referring to Figures 21 through 23. This series of digital images and X-ray maps, which start at a magnification of 30X and then increase to 100X and 250X, respectively, clearly indicate that the void system is inundated with sulfates. In fact, each increase in magnification simply shows smaller and smaller air voids that have been filled.

Occasionally, sulfates were also found around the periphery of some aggregate particles (see Figure 24). Alkali-silica reaction cannot cause features of this type [8]. Instead, these types of features are normally attributed to a cement paste matrix that has expanded (possibly due to frost damage or sulfate related reactions [8]). Such features may also be attributed to poor consolidation during field construction.

Sometimes the cracking pattern around air voids has suggested that expansion has taken place within the air void (see Figure 25). These voids are typically filled with ettringite, as was noted by Marks and Dubberke [3]. Such features suggest that secondary ettringite formation contributed to the microcracking. However, an alternative interpretation of the feature can be formulated. Such an interpretation would maintain that the void had become filled with water and then subjected to freezing and thawing. Hence, the cracks were generated by the expansion of water and then the ettringite precipitated in the void. This alternative interpretation fails to account for the fact that the cracks remain empty while only the air void has been filled with ettringite, such preferential filling seems odd under such circumstances.

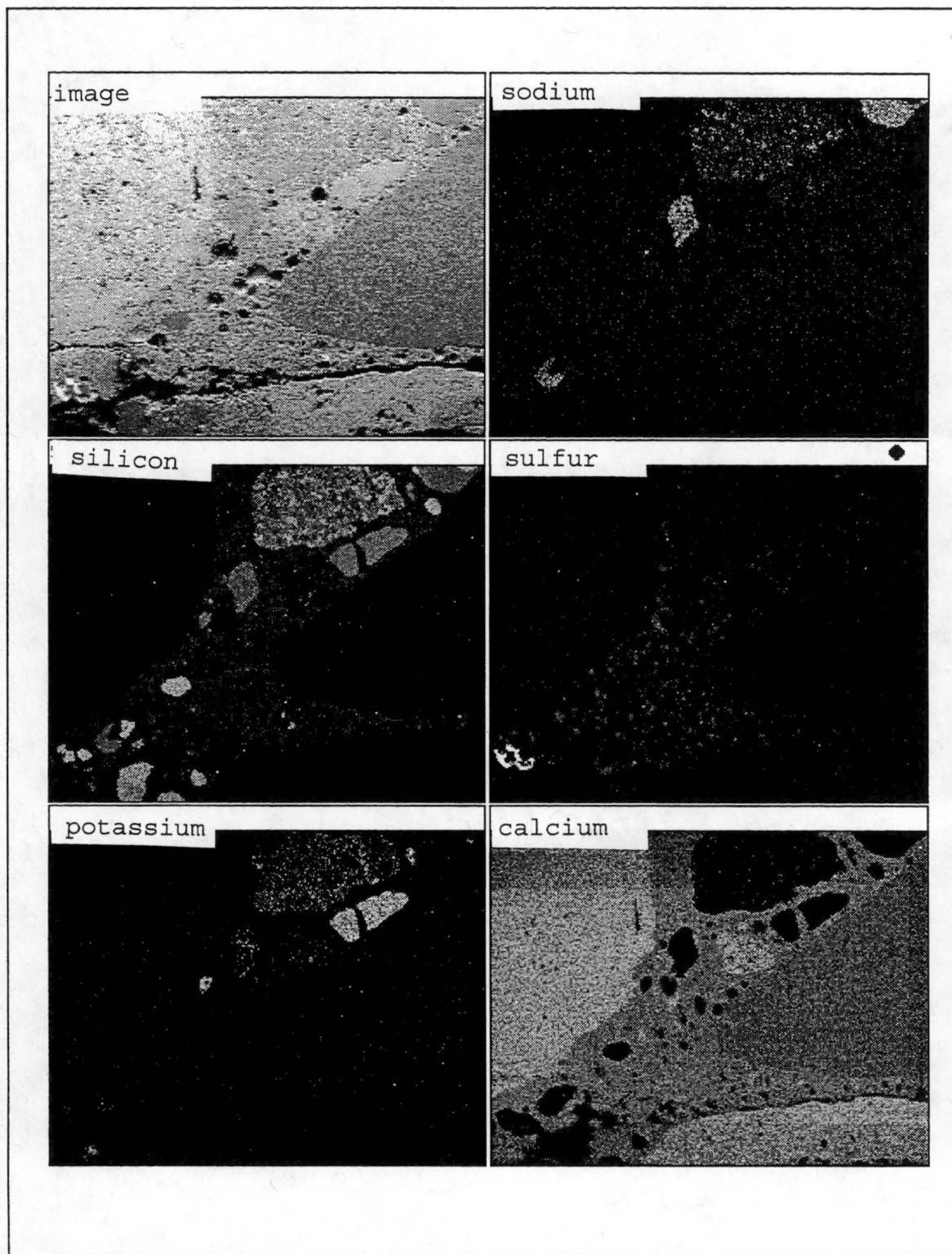


Figure 21. Digital image and X-ray map (magnification =30X) of a large crack in a core taken from I-35. Note voids filled with sulfates (i.e., the sulfur map).

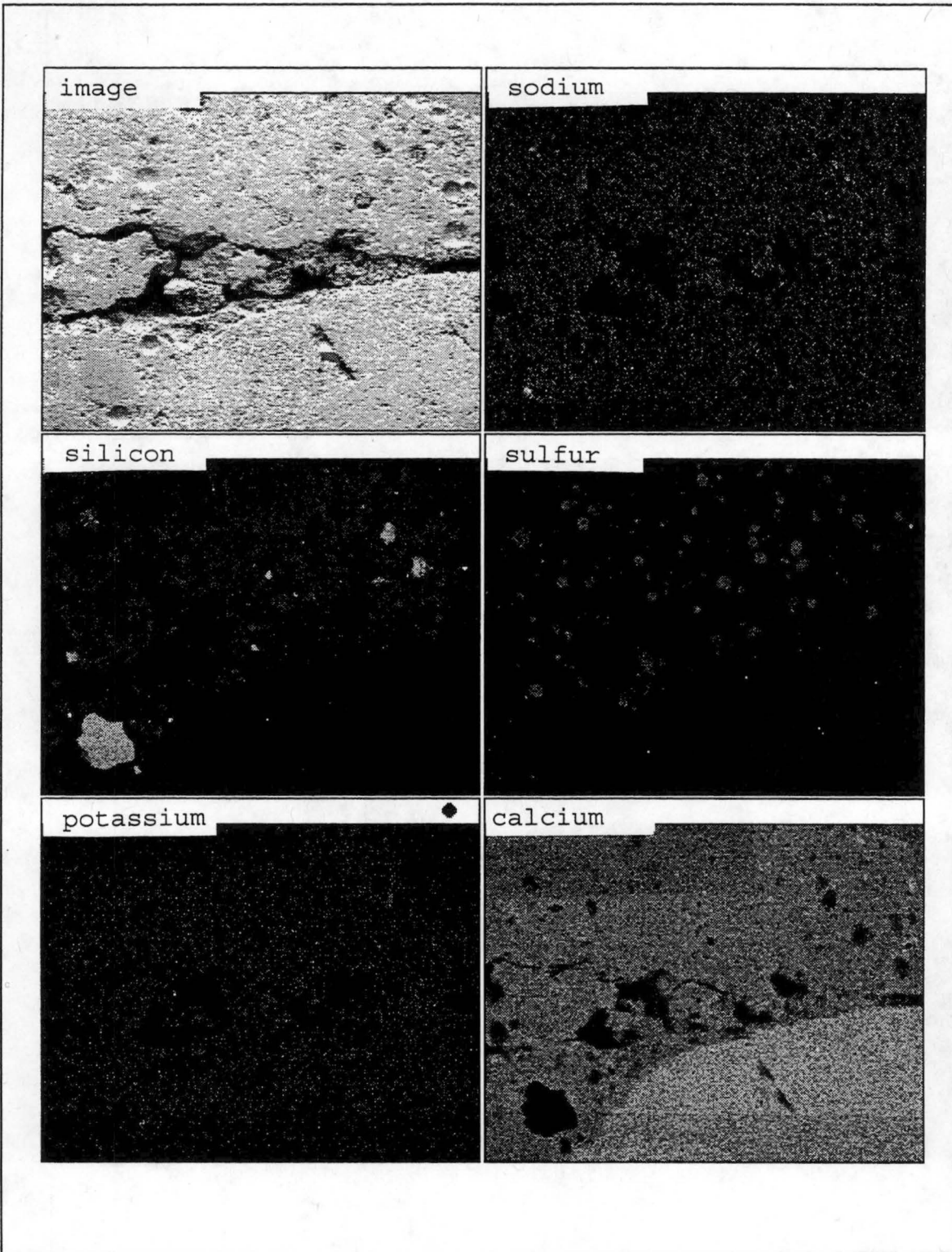


Figure 22. Digital image and X-ray map (magnification =100X) of a large crack in a core taken from I-35. Note voids filled with sulfates (i.e., the sulfur map).

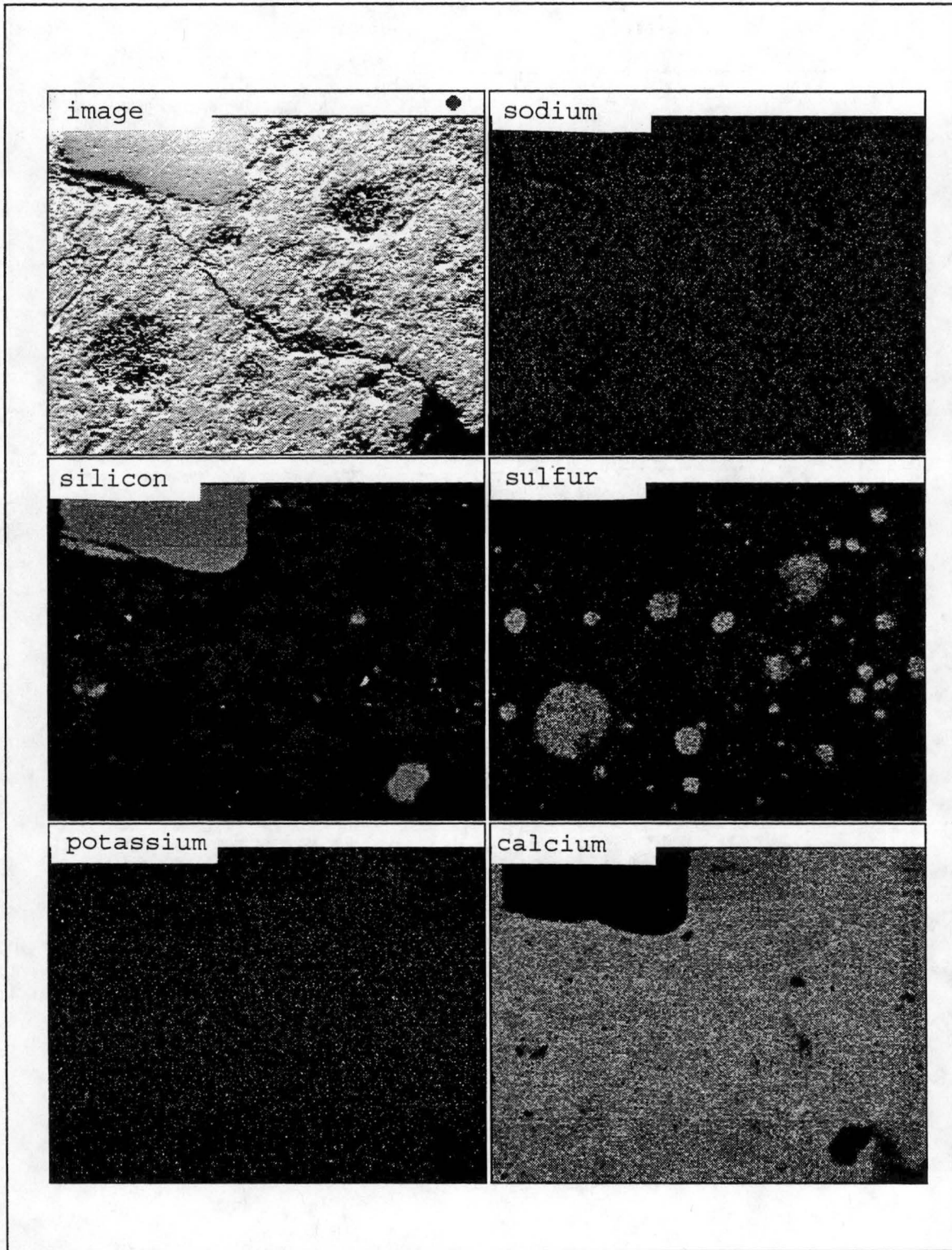


Figure 23. Digital image and X-ray map (magnification =250X) of an area from a core taken from I-35. Note voids filled with sulfates (i.e., the sulfur map).

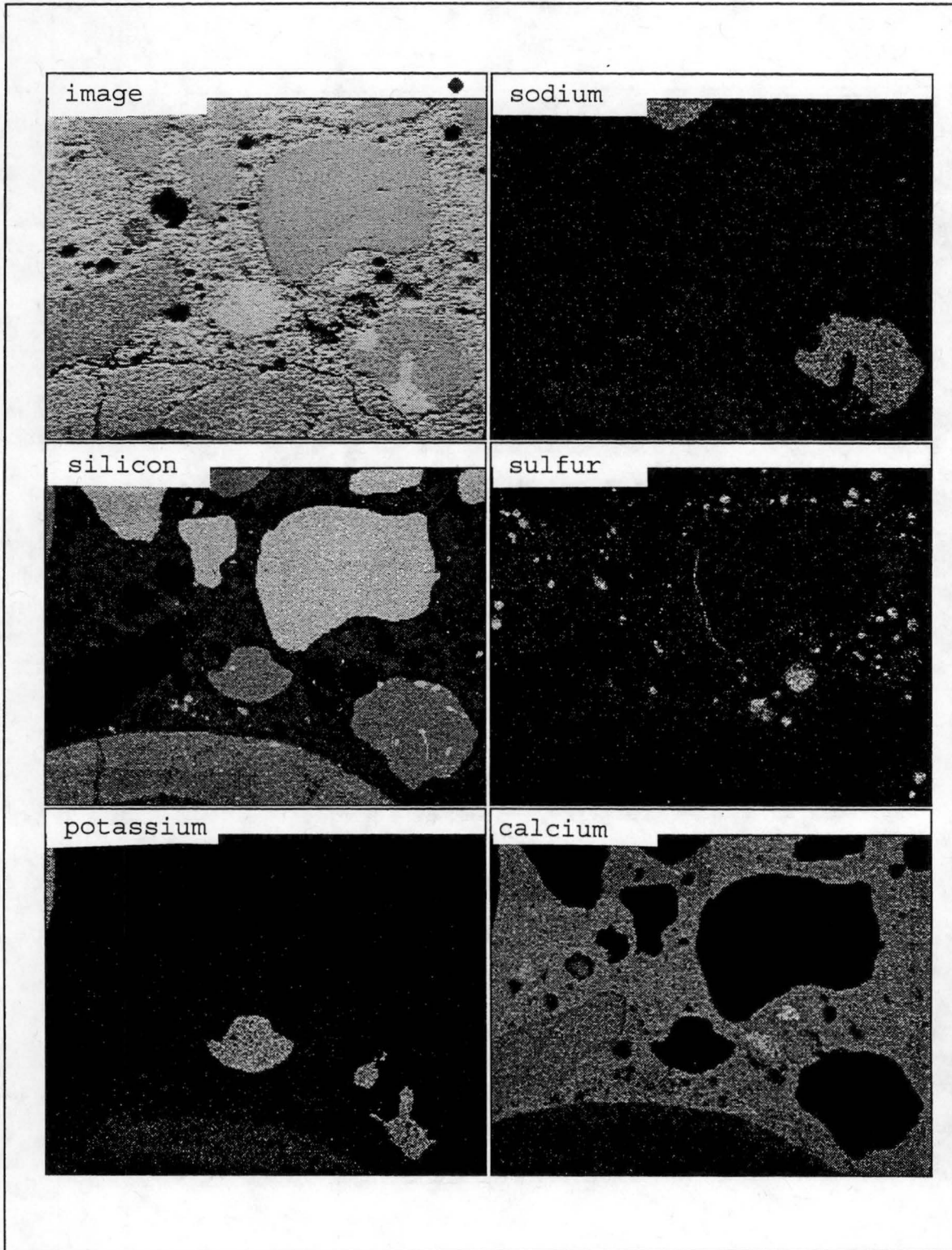


Figure 24. Digital image and X-ray map (magnification =70X) of an area in a core taken from I-35. Note filling around aggregate with sulfates, plus void filling.

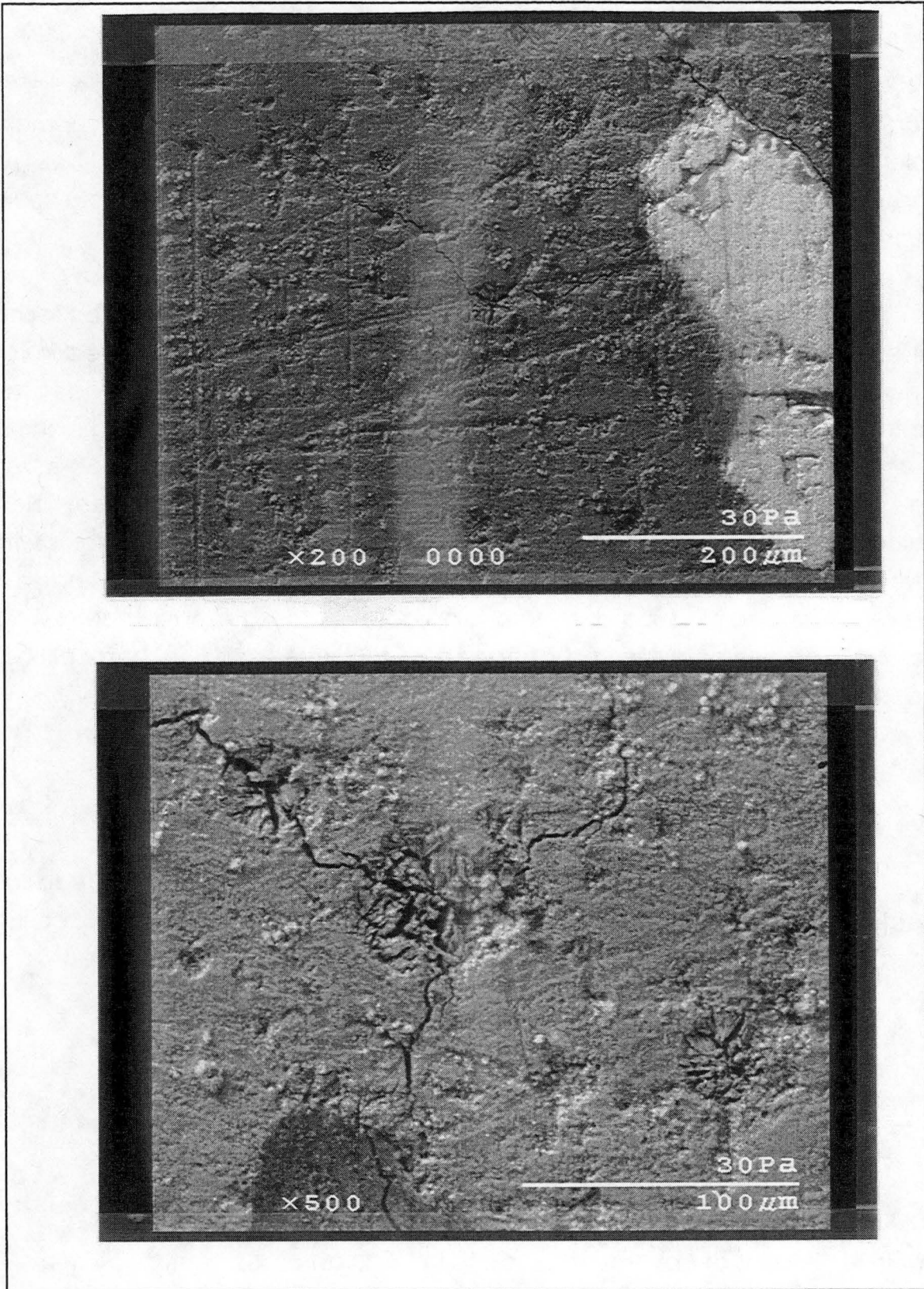


Figure 25. Illustration of cracking patterns through (or from?) air voids in the core specimens.

## SUMMARY

The second year of the project has been spent preparing and analyzing concrete and mortar specimens. Progress was delayed due to equipment problems and delays in getting major equipment orders delivered on time. All of the equipment related details have been resolved and the project should be finished on time.

Currently about 20% of the core specimens have been analyzed. These preliminary studies have produced little evidence of alkali-silica reaction in the samples. All of the alkali-silica gel that was observed has been located in (or near) shale particles. Typically, the cracking pattern that was observed in the samples tended to follow the periphery of aggregate particles; and hence, few aggregates exhibited distress. One feature that was consistently observed in the core specimens was the presence of sulfate minerals in the voids, especially the entrained air voids. The severity of the filling of the air voids with sulfate minerals varied considerably from sample to sample. It is not known if the presence of the sulfate minerals indicates that the pavements were excessively porous and allowed easy access for water or if the cementitious materials themselves contributed to the problem.

## ACKNOWLEDGMENTS

We would like to thank all of the people who helped to contribute to this project. A special thanks to Iowa DOT personnel who spent many days coring roadways to produce the samples that have been analyzed in this project.

## REFERENCES

1. Deicer Distress, by S. Wolter, T.E. Swor, R.D. Stehly and M. Lukkarila; personal communication by R.D. Stehly, 1991.
2. Investigation of Pavement Cracking in US 20 and I 35, Central Iowa, by D. Stark, CTL, Sept. 1992.

3. V. Marks and W. Dubberke, Investigation of PCC Pavement Deterioration, Interim Report for Iowa DOT Research-Project HR-2074 January, 1995.
4. Schlorholtz, S. and K. Bergeson, Evaluation of the Chemical Durability of Iowa Fly Ash Concretes, Final report HR-327, ISU-ERI-Ames-93-411, March, 1993.
5. Emmons, P.H., Concrete Repair and Maintenance Illustrated, R.S. Means Company, Inc.: Kingston, MA, 1994.
6. American Society for Testing and Materials, Annual Book of ASTM Standards, Vol. 4.02, ASTM:Philadelphia, 1994. See C 33 and also C 294, C 295 and C 856.
7. British Cement Association, The Diagnosis of Alkali-Silica Reaction, Second Edition, Wexham Springs, Slough, 1992.
8. Johansen, V., Thaulow, N., and Skalny, J., "Simultaneous presence of alkali-silica gel and ettringite in concrete," *Advances in Cement Research*, Vol. 5, No. 17, 1993, pp. 23-18.
9. Day, R.L., The Effect of Secondary Ettringite Formation on the Durability of Concrete: A Literature Analysis, Portland Cement Association Research and Development Bulletin RD108T, PCA, 1992.
10. Struble, L. and P. Stutzman, "Epoxy Impregnation of Hardened Cement for Microstructural Characterization", *Journal of Materials Science Letters*, Vol. 8, ,1989 pp. 632-634.
11. Stutzman, P. and J. R. Clifton, Microstructural Features of Some Low Water/Solids, Silica Fume Mortars Cured at Different Temperatures, NISTIR 4790, National Institute for Standards and Technology, Gaithersburg, MD, April 1992.

12. Stark, D. Handbook for the Identification of Alkali-Silica Reactivity in Highway Structures, SHRP C/FR-91-101, Washington, D.C., 1991.
13. Idorn, G.M., "Expansive Mechanisms in Concrete," Cement and Concrete Research, Vol. 22, No. 6, 1992, pp. 1039-1046.